Climatic signals and frequencies in the Swedish Time Scale, River Ångermanälven, Central Sweden

Sander, Mikkel

2003

Citation for published version (APA):
Sander, M. (2003). *Climatic signals and frequencies in the Swedish Time Scale, River Ångermanälven, Central Sweden.* [Doctoral Thesis (compilation), Quaternary Sciences]. Quaternary Sciences, Department of Geology, Lund University.

Total number of authors:
1

LUNDQUA Thesis 49

Climatic signals and frequencies in the Swedish Time Scale,
River Ångermanälven, Central Sweden

Mikkel Sander

Avhandling

Lund 2003

Lund University, Quaternary Geology, Department of Geology

Contents

Abbreviations used

AAWP	Average Accumulated Winter Precipitation
AWP	Accumulated Winter Precipitation
CWP	Contemporary Warm Period
DACP	Dark Ages Cold Period
GFF	Geologiska Föreningens i Stockholm Förhandlingar
LIA	Little Ice Age
MWP	Mediaeval Warm Period
NAO	North Atlantic Oscillation
P	Precipitation
Q	Discharge
Qmax	Maximum Daily Annual Discharge
RWP	Roman Warm Period
SMF	Snowmelt flood
SNR	Signal to Noise Ratio
STS	Swedish Time Scale
T	Temperature

[varve] older spelling [*hvarf*, *hvarfvig lera*] *noun*,
Etymological from old-Nordic meaning cycle, circle, periodical iteration of layers.

Climatic signals and frequencies in the Swedish Time Scale, River Ångermanälven, Central Sweden

by
Mikkel Sander

This thesis is based on three papers (I–III), a separate historical paper (IV), a figure appendix (V) and the present synopsis. Appendixes I–III are intended for wider publication. App. IV was written for publication in this thesis only. Appendix V is compiled as a support for the synopsis. I am first author of all papers. First authorship implies responsibility for text, data, analysis, illustrations conclusions and ideas presented, with the following exceptions: (i) Björn Holmquist designed and programmed most of the Matlab tools. (ii) Ingemar Cato provided the varve data from Ångermanälven. (iii) Barbara Wohlfarth and Svante Björck provided additional varve data from River Ångemanälven. (iv) Barbara Wohlfarth provided meteorological data.

Appendix I: – **Sander, M., Bengtsson, L., Holmquist , B., Wohlfarth, B. and Cato I. 2002:** The relationship between annual varve thickness and maximum annual discharge (1909–1971). Journal of Hydrology, v 263, pp 23–35.

Appendix II: – **Sander, M., Holmquist, B., Wohlfarth, B. and Cato, I. 2002:** A 2000 year long record of snowmelt flood derived from a clastic varved sequence and its relation to snowpack changes in central Sweden. Manuscript.

Appendix III: – **Sander, M., Holmquist, B., Snowball, I. and Cato, I. 2002**: Periodicities in the varved record of Ångermanälven: Evidence for solar and atmospheric forcing? Manuscript.

Appendix IV: – **Sander, M. 2002:** A historical review of the "Swedish Time-Scale" (STS): construction and application.

Appendix V: – **Sander, M. 2002:** Figure appendix

1.0   Preface

The thesis represents a synopsis of three articles, plus additional analyses. After presenting some background information in chapters 2–4, the contents of the three articles are summarised in a popular form. Further analyses and data set comparisons, which could not practically be included in the articles are also presented. The additional analyses contribute to the Swedish Time Scale (STS) "missing" varve problem. The articles are presented in App. I–III. In App. IV, I discuss the older literature on the STS, which is beset with controversies and poor scientific reasoning. This appendix is a chronological discussion of the literature on the STS 1884–1940 and some selected papers from the period 1941–1984. In App. V, the numerous cross-correlations and frequency analysis are collected.

2.0   Introduction

Anthropogenically forced climate change, such as that predicted to occur through fossil fuel burning, will be superimposed on the natural variability of the climate system (Bradley and Jones, 1993; Mann *et al.*, 1998). Compared to glacial- interglacial- glacial transitions the climate of the Holocene was considered relatively stable. Considerable evidence, however, has mounted for significant Holocene climate variability at a global scale, even during the late Holocene (c. the last 2,000 years) (Bianchi and Mc-Cave, 1999; McDermott *et al.*, 2001). An important and frequently asked question by international environmental research programmes is: To what extent are the observed high temperatures, extreme precipitation events and apparently more frequent floods an expression of extreme events within the normal variation and to what extent are they due to "human forcing"? The only way to address this question is through the analysis of records from times when human disturbance was insignificant. If the natural variation can be identified and separated from anthropogenic climate forcing it may be possible to understand and manage the changing climate system.

In Europe the longest instrumental meteorological records extend back to the mid 1600's (Lamb, 1977). In the absence of preferred instrumental data (e.g. temperature and precipitation) there are two other types of evidence for past climate variability during the Holocene, (i) historical archives often describing extreme environmental conditions, including diseases and (ii) geological records. This thesis focuses on a specific type of geological archive in Sweden, namely clastic varves.

Due to the short period of the instrumental series, quantitative paleo-climate proxies have to be sought to extend our knowledge of past climate variability in the long-term geological perspective (e.g. Mann *et al.*, 1999). One of the shortfalls of quantitative paleo-climatic proxies is that the relationship between climate parameters and the measured proxies are not necessarily stationary over time. The variation that the proxies possess during and beyond the period of instrumental data may not be controlled to the same degree by the forcing parameter e.g. reduced sensitivity of recent tree-growth to temperature at high northern latitudes (Briffa *et al.*, 1998b). Despite calibration against instrumental data, there is no guarantee that a mathematical relationship (a so called "transfer function") used to convert a specific geological proxy into a climatic variable has remained constant over time and space.

A wealth of tree-rings series from the high latitude Northern Hemisphere provide firm evidence for the existence of a Medieval Warm Period (MWP) (c. 1000–1300 A.D.) (Crowley and Lowey, 2000; Esper *et al.*, 2002). In addition, historical documents tell that climate was considerably warmer during the MWP than the preceeding and subsequent periods (Lamb, 1977). However, can the Medieval Warm Period be compared to the present warming trend and to what extend may the contemporary warming since the early 1900's in Europe simply reflect a natural "recovery" from the cold Little Ice Age? It has been suggested that the last decade of the last millennium was the warmest on the Earth for the last 1,000 years, but even so, was it the warmest of the last 2,000 years? Is the present centennial-scale warming trend extraordinary, or is it within the range of previous climate shifts that took place during the Holocene? Although contemporary warming has been observed in many places of the world (Watson and Coregroup, 2001), Greenland, for example, has undergone a recent cooling trend (Cappelen, 2002). The oxygen isotope composition of the Greenland and Antarctic ice-sheets have been compared to each other as "hemispheric thermometers" over glacial-interglacial cycles, but there has so far been only limited interpretation of the Holocene sections of these unique records, despite the annually resolved nature of the ice-core chronologies.

In the context of future climate change, the most profound impact on humans and society is likely to be caused by rearrangement of the hydrological cycle (Milly *et al.*, 2002; Palmer and Räisänen, 2002; Watson and Coregroup, 2001). Changes in precipitation, evapotranspiration and groundwater levels will significantly influence agriculture and populations, near major rivers (Watson and Coregroup,

2001). Despite the initiative to reduce CO_2 emissions the associated greenhouse effect is still increasing and a steady increase of atmospheric CO_2 concentration due to future consumption of fossil fuels is expected (Watson and Coregroup, 2001). Given that this predicted change in atmospheric CO_2 level will lead to a warmer Earth, the hydrological cycle will intensify, more water will be cycled between the oceans, atmosphere and landmasses. However, in areas where evapotranspiration exceeds that of increased precipitation drought is expected to occur (Watson and Coregroup, 2001). Modelling future run-off for climate change scenarios normally involves a temperature increase in the range from $1–4°C$ and a net annual increase in precipitation by 10–30% e.g. (Bengtsson and Iritz, 1990; Gleick, 1989; Panagoulia, 1991; Xu and Halldin, 1997).

Extending a record of the hydrological cycle in northern Sweden, beyond the range of instrumental data, forms the focus of this thesis. A relatively simple theory, based on hydrological modelling of discharge responses to climate changes (e.g Bengtsson and Iritz, 1990; Gleick, 1989) suggests that, in a warmer northern Sweden, the strength of the snowmelt flood (SMF) will decrease due to a reduction in the amount of solid winter precipitation (as winter becomes shorter). At the same time, the number of autumn storms and associated floods will likely increase, as will total annual river discharge. These changes will influence the return time (or period) of extreme floods and river flow in general. This thesis and the articles presented herein give a rare glimpse into the variations within a long proxy-record of river discharge and the factors forcing it.

This thesis focuses on the clastic varve thickness measurements that form the basis of the STS and the relationship between varve thickness, instrumentally recorded river discharge and meteorological parameters. The relationship between varve thickness and discharge variation has been scrutinized and several models (linear, logarithmic and power) relating the two data sets tested. A power model was singled out as the best performing model and subsequent applied to the c. 2000 year long record of geometric mean varve thickness, thus transforming varve thickness variation into discharge variation. Discharge variation is subsequently compared to a suite of alternative climate proxies (e.g. tree-rings, NAO, geostrophic wind, vorticity, maximum Baltic sea-ice extent, volcanic eruptions and ^{14}C production rates).

The STS is a well-established varve chronology, at least for the relatively recent past (i.e. the last 2000 years) and it is tied to the present through modern varve sediments obtained from the River Ångermanälven estuary (Cato, 1987). Therefore, the most recent part of the STS was formed within the range of instrumental meteorological observations. The connections between several individual varve segments have been statistically verified by cross-correlation analysis (Wohlfarth *et al.*, 1998) and the overlaps allow the calculation of a geometric mean, which gives a more precise estimate of varve thickness variability. In its composite form the varve chronology is well suited for testing the potential relationships between varve thickness and climate related meteorological and hydrological observations, particularly as it is fixed to the present day.

The movement of water in River Ångermanälven, which controls sediment transport and deposition (and hence varve formation) is controlled by precipitation (P), temperature (T) and the catchment's geographical /physical conFig.uration. Thus, the variation in observed discharge can be hydrologically modelled using daily P and T series as input data (Bergström, 1992) and varve thickness could be calculated using a sediment transport equation (Sander *et al.*, 2002; Nilsson, 1972). However, the paleo-perspective requires the opposite solution; past temperature and precipitation are to be reconstructed from the varved record. This is a cascading inversion problem, where a single proxy variable (in this case varve thickness) is controlled by two (or more) forcing agents and the relationships between the (>) two forcers and the proxy may vary through time. Although this problem is common, it is frequently omitted from studies of the reconstruction of quantitative data from paleo archives.

2.1 Varves

2.1.0 Varve formation

Varves can be divided into two main forms: clastic and biogenic. Clastic varves are mainly allochthonous, biogenic varves are mainly autochthonous, both types occur mainly in sedimentary environments where (semi) permanent stratification exists (O'Sullivan, 1983; Petterson, 1999; Saarnisto, 1986). The sedimentary processes that lead to the formation of annually laminated clastic or biogenic sediments are driven by the seasonal cycle. Clastic varves are frequent in peri- and semi- glacial environments and numerous sequences are found in Arctic Canada, Sweden and Central Europe (e.g. Lamoureux, 1999; Lidén, 1913; Leemann and Niessen, 1994). In Fennoscandian lakes the varve couplets are frequently composed of equal amounts of clastic and biogenic material (Petterson *et al.*, 1999; Snowball *et al.*, 2002). The fluvial varves of River Ångermanälven

and other Swedish rivers are also clastic, as are those that comprise the entire STS. Biogenic varves are most frequent in European (Maar) lakes (Zolitschka, 1992; Zolitschka *et al.*, 2000). In marine basins and Fennoscandian lakes the varved sequences often have a biannual contribution from the two sources: clastic and biogenic. The varves in the Cariaco basin have a clastic component from the monsoon, which increases river influx, and a biogenic component due to biological production (Hughen *et al.*, 1998).

The influx of materials to the majority of sedimentary basins (with the possible exception of the deep ocean) varies according to the seasonal cycle. However, the sedimentary record of the seasonal cycle is frequently destroyed by bioturbation, i.e., the physical reworking of the upper sediment layers by burrowing animals. Therefore, the most important factor for the preservation of varves is the absence of a bottom-burrowing fauna and in the majority of systems this lack of substantial life is caused by constant or discontinuous anoxia. The preservation of clastic varves in River Ångermanälven is due to anoxic conditions, which are continuous in the deepest parts and discontinuous in the entire Kramfors basin (Cato, 1987).

The internal layering of varves has traditionally been named "summer" and "winter" because of the origin of terminology in glacial deposits (De Geer, 1940). Enhanced melt water generated from the ice sheet during the peak of summer forms a coarse "summer" layer and settlement of fine particulate material during the ice stratification forms a "winter" layer. In the case of post glacial varves the coarse layer formation is not at the peak of summer but in the spring. The fine layer is still deposited under intense stratification during winter. Thus it seems more reasonable to speak of a "spring" and "winter" layer.

2.1.1 Paleo-climate studies of varves

Varves have been utilized mainly in circum-arctic regions as a paleo-climatic archive. For example, the thickness of varves in a glacial fed lake reflects the amount of melt-water released during the summer, and may be related to summer temperature (Perkins and Sims, 1983). At temperature $>0°C$ snow and ice melt; in a system where the supply of ice and snow is unlimited the amount of melt-water produced is proportional to temperature. The melt-water acts as a medium for sediment transport and thus greater melt-water release leads to thicker varves. In some oligotrophic lakes, catchment discharge transports nutrients in solute form into the water column, which leads to increased primary production and hence precipitation forms the main governor of varve thickness (Lotter, 1997).

2.2 The Swedish Timescale (STS)

The STS is compiled from thousands of varve sections along the Swedish east coast (Wohlfarth and Possnert, 2000) and it forms a chronology with annual resolution that covers the Holocene and extends into the Late Glacial (Cato, 1987; Cato, 1998; De Geer, 1912; Strömberg, 1985). Based on the geographical location of the varves the STS was initially divided into four parts; the dani-, goti-, fini- and post glacial. The dani glacial (Hansen, 1940) period was later discarded because of problems concerning the internal connection of the dani glacial and, more importantly, the failure to connect the dani glacial to the goti glacial (De Geer, 1926; Milthers, 1927).

Varve deposition followed the northwards receding Scandinavian ice sheet. Thus, the southern varves are oldest and the northern varves are youngest. The division of the STS into goti- and fini glacial varve series is based upon a major still stand of the ice front during the Younger Dryas, at times when the ice front was situated in the Baltic Sea or its ancient equivalent (Björck, 1995). The post glacial varve series marks the period after the catastrophic drainage of an ice-dammed lake, that lead to the bipartition of the ice-sheet (Borell and Offerberg, 1955).

The STS facilitated the establishment of the first deglaciation chronology many years before the advent of radiometric dating (De Geer, 1912). Even in its earliest form the STS also allowed for a reconstruction of the ice front positions and recession rates. The chronology has been extended and revised many times (e.g. Strömberg, 1985), but despite these efforts it is still claimed that a considerable number of varves (c. 500 years) are missing (Wohlfarth and Possnert, 2000). The early literature dealing with the construction of the STS is presented in App. IV. An analysis of the continuing missing varve problem in the post glacial is presented in chapter 7.

2.3 Assessment of floods

For any hydro electrical construction it is necessary to assess the dimension of the most extreme flood with in a given period, because such constructions represent a considerable investment and because dam failure can lead to catastrophic flood in the downstream area. Dam failures can result in the most damaging flood events. When a dam fails, a gigantic quantity of water is suddenly let loose downstream, destroying anything in its path. For example, in 1889, more than 2,200 lives were lost as a result of the Johnstown, Pennsylvania flood caused by an upstream dam failure. (http://www.abag.ca.gov/bayarea/eqmaps/damfailure/damfail.html).

If a construction is to stand for 200 years then some assessment of the expected 200-year flood must be presented. Since natural observed flow on time scales longer than c. 100 years are absent in most watersheds long return time floods must be estimated by either discharge models or statistics on the short observed record.

Through flood frequency analysis, the discharge records and models of extreme floods in Swedish rivers have been studied in great detail e.g. (Harlin, 1992; Lindström, 1993). The probability distribution of discharge data allows for an assessment of the intensity of floods or a statistical statement to be made about the return time of floods. Based on a limited number of observations (e.g. 100 years of data) it is possible to assess the return time of a flood of specific height, assuming that floods of longer return times are related, via a scaling factor, to those observed. Such predictions are an essential part of the design of dams built for hydro-electric power purposes and other constructions in rivers that are required to withstand extreme floods events, which perhaps have never been observed, but can be anticipated within a given time frame.

Given a series of extreme floods, the occurrence of the most extreme flood event can significantly influence the size of predicted return floods and their return times. This influence is due to the fact that the prediction is solely based on a scaling of the observed record and any substantial changes in the mean and standard deviation of the observed record will modify the numerical value of a flood predicted return period. For example, the distribution of extreme high water along the Danish west coast was significantly modified by one high water event caused by the hurricane of 1999 A.D. This event meant that dikes originally designed to withstand the 500-year spring tide would not protect against the expected 90 year high water (Gammelgaard, 2001). In such cases, geological data is required to provide a more accurate estimate of the return time of extreme events.

Due to the short temporal range of instrumental discharge measurements (1909 A.D.–present for River Ångermanälven) little is known about the return time of floods at greater than centennial timescales. It is one of the aims of this thesis to present the geological assessment of floods with long return times based on the analysis of varve thickness. The prerequisites for a robust reconstruction are manifold. The most important are (i) a robust annual chronology for the varve thickness (ii) that the internal variation geometric mean varve thickness record is a true proxy for the variation in annual sediment transportation, (iii) that the relationship between discharge and geometric mean varve thickness

does not change through time. The latter assumption requires that the discharge that dominates channel morphology, often referred to as bankfull discharge (Richards, 1982) has not changed over the time period in question.

3.0 The River Ångermanälven Catchment

3.1 Geography

The province of Ångermanland, which covers an area of 19.800 km^2 is located in central Sweden. "Ånger" is derived from the Norwegian word "Anger", which translates into "deep bay" and refers to the estuary. The province of Ångermanland more or less corresponds to the River Ångermanälven watershed. Sollefteå (population c. 9000) is the major city within the watershed of the River Ångermanälven catchment. Located outside the catchment, but inside the province, the towns of Härnösand (population c. 30.000) and Örnsköldsvik (population c. 60.000) are the main cities. Large pine and birch forests cover most of Ångermanland, which supply raw materials for an extensive timber and paper industry (Carlgren *et al.*, 1925). Extensive fishing of salmon was previously an important industry in the River Ångermanälven (Arnborg, 1958). Agriculture is limited to the river valleys in the fine-grained postglacial fluvial sediments, often deposited in flood plains that once lay below the highest shoreline (see chapter 3.2). Prehistoric settlements are numerous in the Ångermanland, where Iron Age (Wallin, 1996), Stone- and Bronze Age graves and artefacts are frequent (Olsson, 1914). Extensive petroglyphs fields (Stone Age) were unearthed during dam constructions at Nämforsen. These fields indicate that Ångermanland was an important region both for religious rituals and salmon fishing in prehistoric times.

3.2 Geology

The pre-Quaternary geology of Ångermanland consists of two main genesis belts. To the west lies the Caledonian mountain chain and to the east lies the Sveccofennian orogenesis belt, which are separated by the Caledonian trust front. The Caledonian or "Scandes" mountain chain is dominated by a suite of metamorphic rocks including, e.g., gabbro, amphibole, mica schist and even some eglocite. The Sveccofennian orogensis belt is dominated by granite and pegmatite in the western part, greywacke in the eastern part along with sparse occurrences
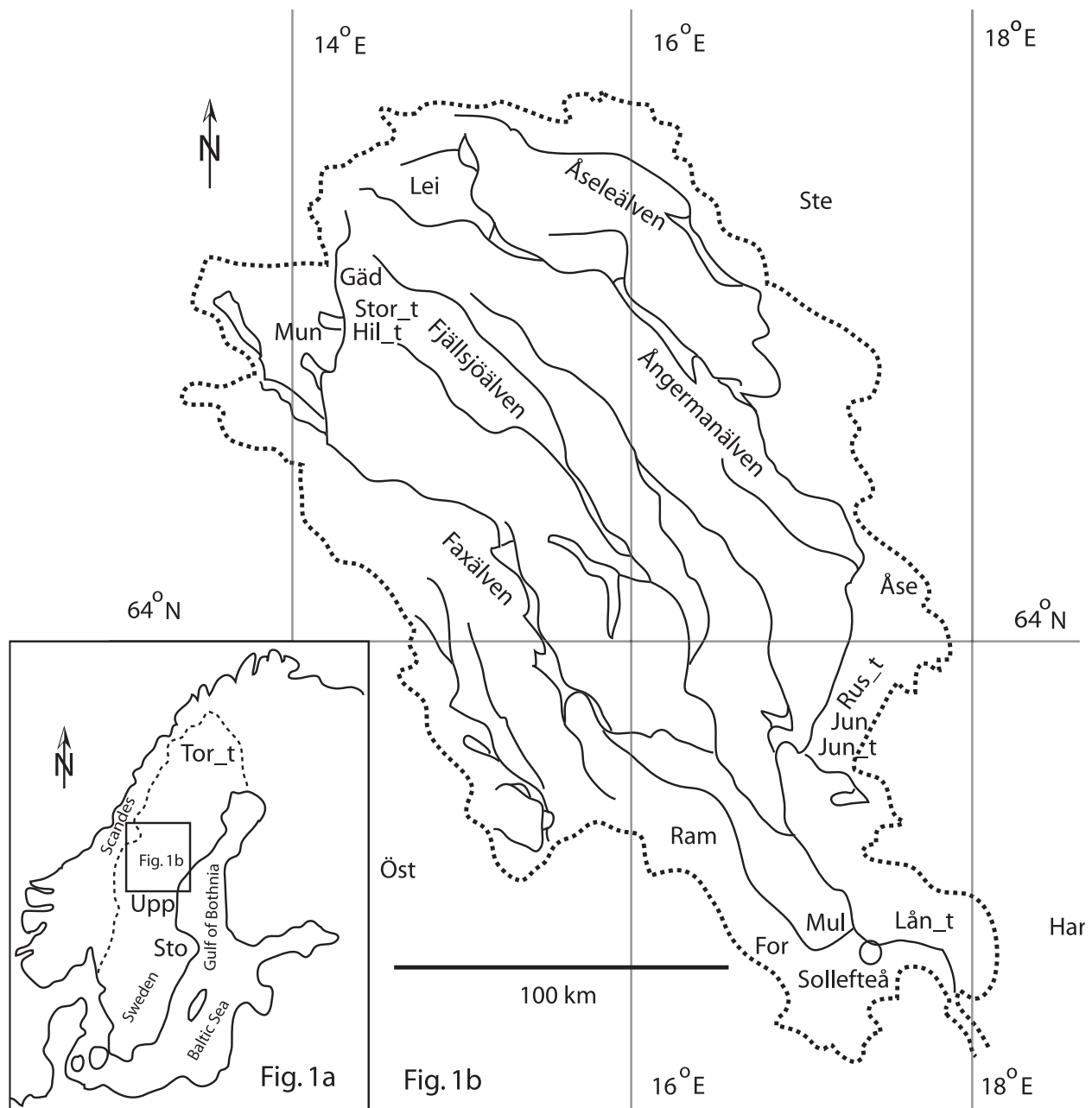
Fig. 1 a. *Fennoscandinavia and the position of River Ångermanälven*
Fig. 1 b. *Catchment of Ångermanälven, Meteorological stations: Gäd – Gäddede, Lei – Leipikvattenet, Mun – Munsvattenet, Jun – Junsele, For – Forse, Mul – Multrå, Ram – Ramsele, Åse – Åsele, Ste – Stensele, Öst – Östersund, Har – Härnösand, Sto – Stockholm, Upp – Uppsala, Tree-ring series Tor_t – Tornaträsk, Hil_t – Hillsandhöjden, Sto_t – Storvattenet, Rus_t – Ruskhöjden, Jun_t – Junsele and Lån_t – Långbroberget. Position are approximate, see original publications for exact location (Linderson, 2000; Wohlfarth et al., 1998).*

of syenite, rapakivi and diabase fields and dykes (Fredén, 1994).

The Quaternary cover is dominated by an extensive series of moraines above the highest shoreline and by post glacial fluvial sediments in the river valleys and flood plains below the highest shoreline. Fluvial sediments deposited during the last c. 8000 years can be found in isostatic raised deltas along the river-valleys. The oldest delta sediments were deposited in the

west and the youngest in the east. An estimate of the isostatic uplift was used by R. Lidén to approximate the number of varves deposited sub-aquatically in the present delta (Lidén, 1938). Later a more reliable value for the isostatic uplift (8.0–8.5 mm year^{-1}) was calculated based on old watermarks, (Bergsten, 1954). Recently more sophisticated numerical models of the ice sheet, crust and lithosphere estimates the uplift to 7 mm year^{-1} (Lambeck *et al.*, 1998).

3.3 Hydrology-Estuary

The drainage basin covers 32,000 km², of which 7.2% is lake surface area (Fig. 1). The river has three main tributaries; Ångermanälven, Fjällsjöälven and Faxälven. The three tributaries originate in the Scandes mountain chain and converge near the Baltic coast, upstream from the town of Sollefteå. The combined water-mass discharges into a narrow estuary, where a substantial delta has formed. Wave action is limited in the narrow estuary and tidal waters are absent in the Gulf of Bothnia, which restrict the reworking of sediments. The delta crest lies approximately 1 m below sea level. Beyond the crest the delta slope sharply dips down to c. 100 m below sea level in the Kramfors basin (Arnborg, 1958; Arnborg, 1959; Cato, 1987). Annual layers in the delta sediments result from the seasonal variation in discharge and these are preserved because of (semi)-permanent anoxia (Cato, 1987).

The maximum annual winter discharge is generally below 300 m³s⁻¹, while the SMF value normally exceeds 2000 m³s⁻¹ (Fig. 2). After the SMF, which lasts a few weeks, discharge returns to lower levels reflecting summer precipitation (Sander *et al.*, 2002). During the autumn the discharge level again raises due to storms and in some years the autumn discharge levels can equal or exceed that of the SMF (Fig. 2).

River Ångermanälven is one of the most extensively regulated rivers in Sweden. Fifteen percent of Sweden's hydroelectric production is produced within the county of Sollefteå and more than 40 dams and other hydro-electric installations have been built

in the River Ångermanälven watershed since the late 1930's (Nilsson, 1972). The purpose of these dams is to store some of the SMF in artificial lakes and reservoirs, for later release when the natural flow would be too low to meet power demands. The influence of hydro-electric installations in River Ångermanälven is clearly visible in the discharge record after 1950 A.D. (Sander *et al.*, 2002). Clear post- and pre-regulation river flood distributions can be identified from the discharge observations. The pre-regulation period is characterized by a significant peak in SMF followed by rather low flow during winter and summer. On the other hand, the managed post-regulation period has a muted SMF peak and increased winter and summer flow.

3.4 Meteorology

River Ångermanälven's watershed can be sub-divided into three landscape zones, which also have different meteorological characteristics, based on the 30 year normal period (1961–1990). The Scandes Mountains in the west rise to 1200 m a.s.l. and have a mean annual temperature between c. –2 and +2°C and a mean annual precipitation of 600–1200 mm (Raab and Vendin, 1995). The central part is a highland (inland) area with altitudes between 500 and 1000 m a.s.l., a mean annual temperature between 0 and +4°C and a mean annual precipitation of around 500 mm (Raab and Vendin, 1995). The coastal zone to the east has a mean annual temperature of c. +4°C and a mean annual precipitation of 600 to 700 mm (Raab and Vendin, 1995). Generally >30% of the
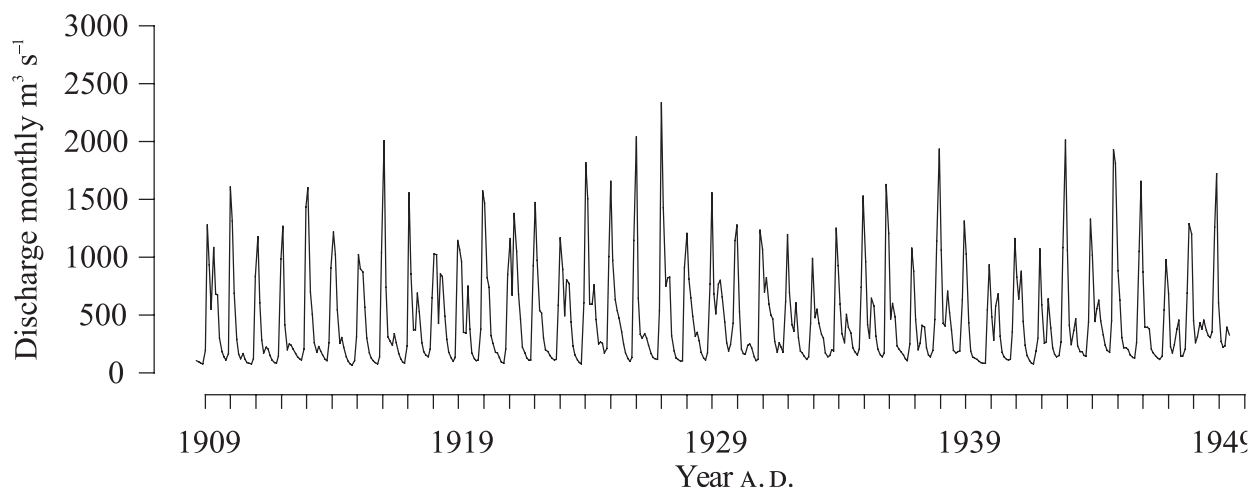
Fig. 2. Monthly discharge variations form the hydrological station at Sollefteå (1909-1950). The period after 1950 is heavily influenced by hydro-electrical dam constructions and does not possess the natural variation of the flow. Winter discharge is low, flow peak in May or June during the snow melt flood in which the maximum daily annual discharge flow normally appears. Autumn flows sometime reach the height of snowmelt but rarely exceeds it, in the observed record it only occurred once 1921. Since monthly flow is averages it does not necessary captures the height of the maximum daily annual discharge.
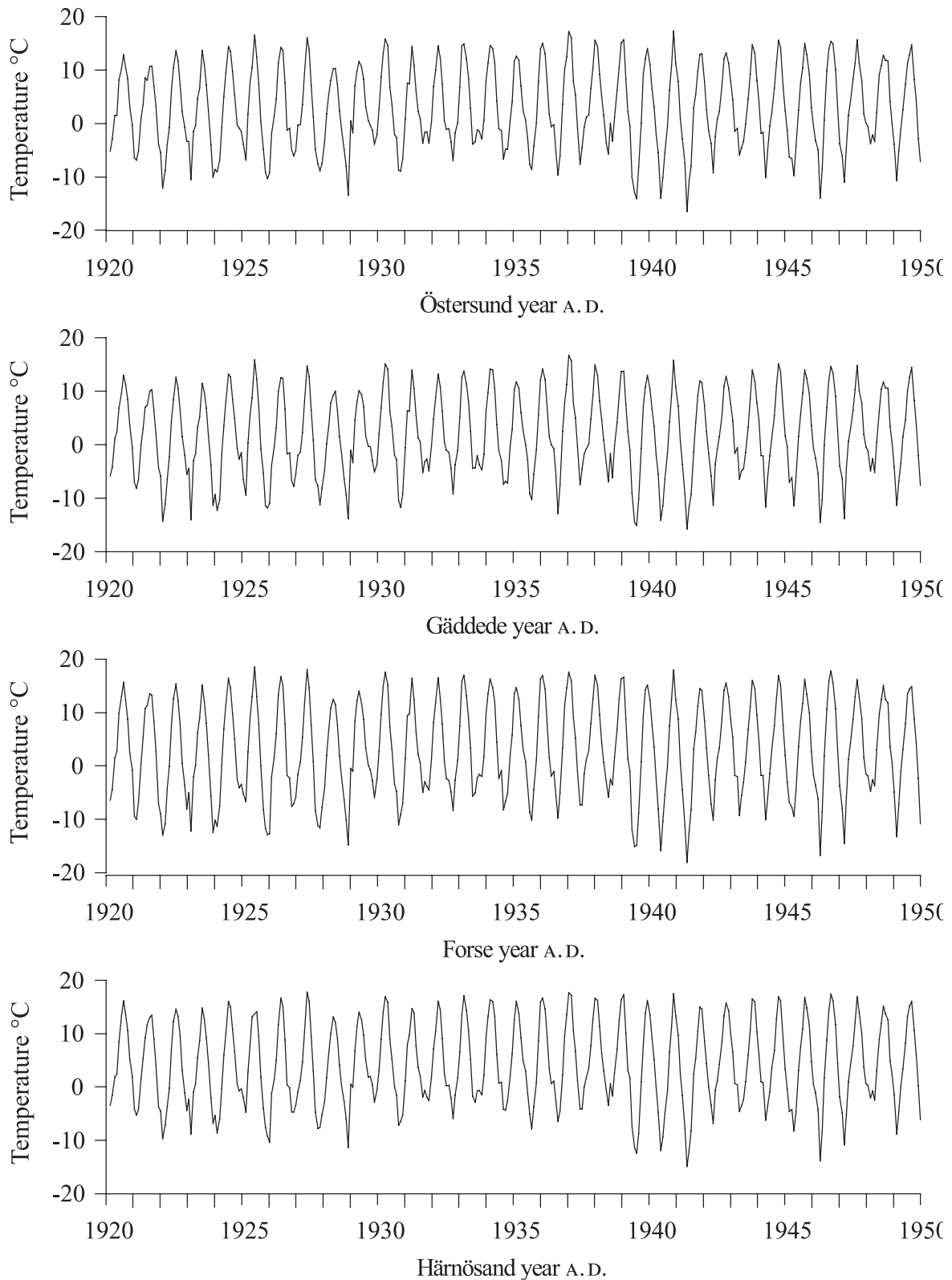
Fig. 3. Monthly temperature variation at four representative meteorological stations, in and near the catchment, 1920–1950 A.D. Showing the seasonal variation in temperature. Note that small changes in temperature are mirrored in most series, i.e. temperature variations are regional.
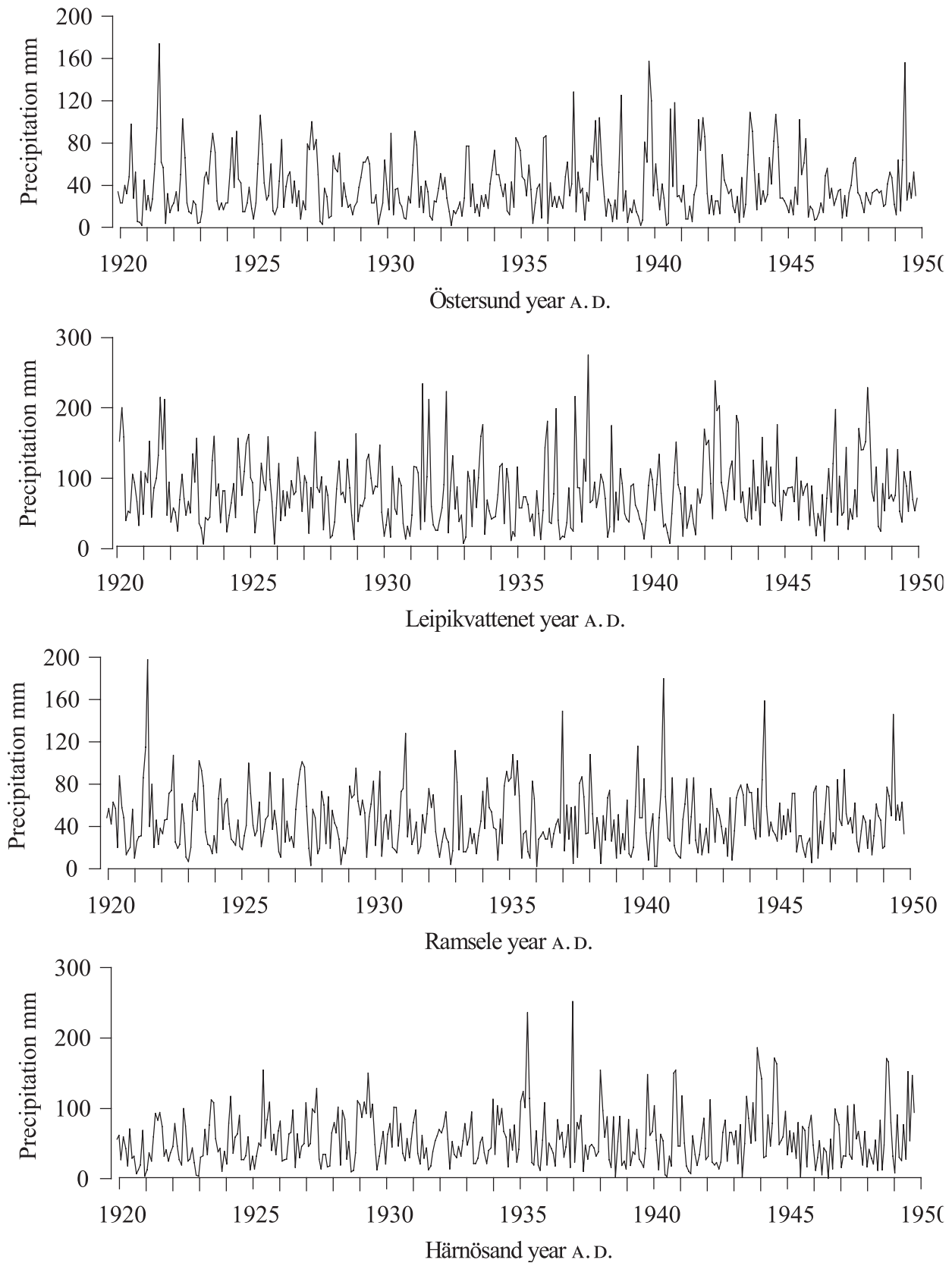
Fig. 4. *Monthly precipitation variation at four representative meteorological stations, in and near the catchment, 1920–1950 A.D. Showing the seasonal variation in precipitation. Note that only a minor part of the variation is shared between the series, i.e. precipitation variations are local.*

annual precipitation in the watershed falls as snow (Raab and Vendin, 1995). The strong seasonality in temperature and precipitation (Figs. 3 & 4) gives rise to a strong seasonal signal in the discharge pattern of river Ångermanälven (Fig. 2).

4.0   Methods

Two types of numerical methods were used (i) cross-correlation and (ii) frequency analysis, both written in Matlab [TM] 5.1 and 5.2 software package. Additional toolboxes, besides those included in the standard version of Matlab were downloaded from various locations. The correlation coefficient (r) was used to analyse the relationship between any two parameters, while the variance explained (r^2) was considered when a relation between two parameters could be defined as causal. There is no mathematical difference between the two, the square of r equals r^2 and the square-root of r^2 equals r, but r is merely descriptive while r^2 is associative. In this thesis only correlations that remained significant at the 95% confidence level are considered to be indicative of a valid relationship between two variables. The correlation coefficient (r) is an expression of the co-variation between two series. A Signal to Noise Ratio (SNR) is the ratio of what is explained divided to what is unexplained $r/(1–r^2)$. Due to the relationship between r and SNR, the present author uses the term "correlation" in a descriptive sense when commenting on the SNR cross-correlation plots.

4.1   Cross-correlation

Cross-correlation is now a standard practice applied to the connection of varve diagrams (Holmquist and

Wohlfarth, 1998). The cross-correlation statistical package utilized here was originally developed for cross-correlation of the fini- and goti glacial varves and the sub-recent part of the STS (Holmquist and Wohlfarth, 1998; Wohlfarth *et al.*, 1998). The cross-correlation exercise followed in this Thesis was taken in three steps; (i) the two records were compared by a series of SNR's or correlation coefficient's (r) as the records were moved in increments of one data point (= one year), (ii) the frequencies at which significant correlation(s) or SNR's were present were calculated, (iii) the sign of correlation was calculated as a spectrum of frequencies. This treatment provides allowance for variation as an inverse correlation sign between the fast and slow frequencies. These three analyses provide a comprehensive overview of all possible correlations between the two data sets considered during any one analysis and shows how the data may be further modified. An example of a cross-correlation is presented in Figure 5.

4.2   Frequency analysis

Two types of frequency analysis have been used, frequency analysis by the periodogram and the Morlet-type wavelet. Frequency analysis by the periodogram is a frequency analysis of fixed periodicities. One hundred frequencies in the 2–N year band (where N=number of observations) were checked in the varve record. Extremely thick varves can dominate the result of the frequency analysis and these were either removed or reduced by log transformation of the data set or other amplitude reducing methods, like various forms of indexing.

The main drawback of the periodogram is the difficulties it has in handling non-stationary frequencies,
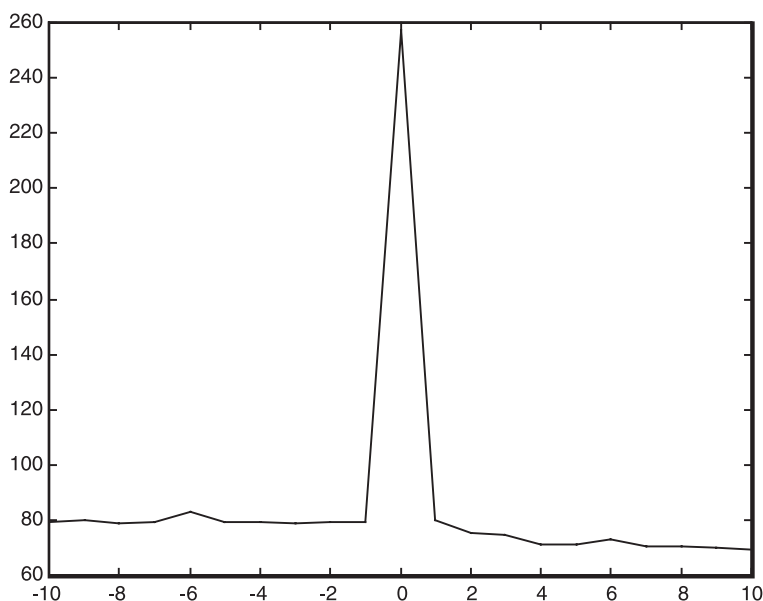
Fig. 5. Example of cross-correlation. The figure shows development of SNRs as the two records are moved with respect to each other. On the x-axis the two record are moved in increments of one data point (e.g. a year or a month). Zero at the center of the x-axis denotes the position of the two records on they respective time scales. To the right and left on the x-axis, respectively positive and negative values denoting lead or lag. Both directions can denote lead or lags it depends solely on the order in which the records are introduced to the calculations. On the y-axis SNRs values are calculated at each increment step. This example has significant SNR is seen as a peak at zero time lag.
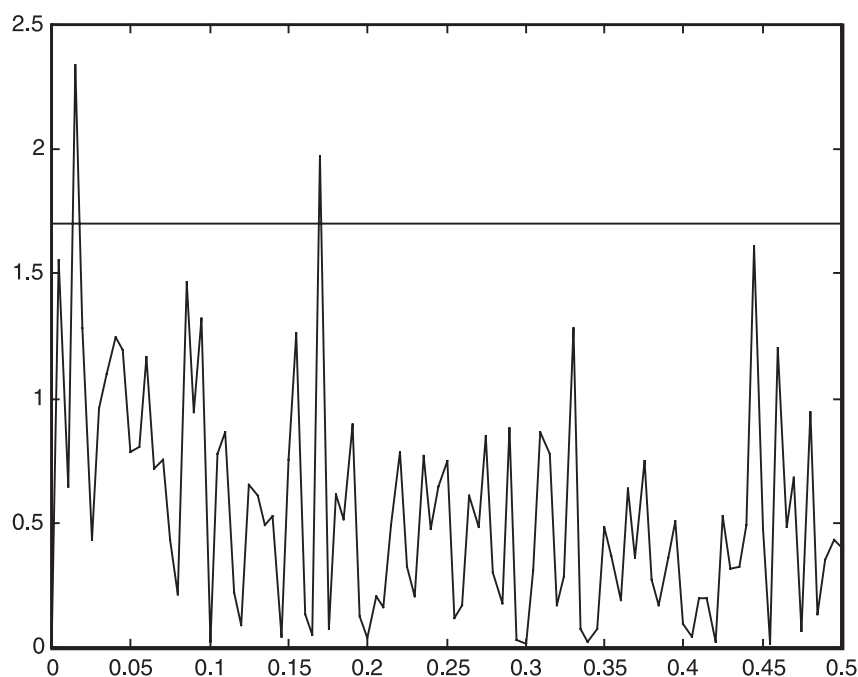
Fig. 6. Example of frequency analysis by periodogram. 100 frequencies in the band from 2 to N years (N = number of observations) is presented on the x-axis. Here the frequency is showed as cycle pr year (e.g. 0.1 cycles pr year equals a 10 year cycle). The significance of each 100 frequencies is calculated, showed on the y-axis. The vertical line is the 95% level.

which are common in paleo-climatic data. In principle a Morlet wavelet analysis can cope with the non-stationary of frequencies as a function of time, but the complexity of the mathematics increases. An example of a frequency analysis is presented in Figure 6.

4.3   The Gumbel distribution

A statistical distribution specially designed for extreme events, the Gumbel distribution, was applied in Paper I. The SMF is such an extreme event, marking the brief high stand of a river each year and the series of maximum daily annual discharge is a series of extreme events. The Gumbel distribution is a special case of the Fisher-Tippett distribution, which is also called the extreme value distribution or the log-Weibull distribution.

5.0   Summary of papers

5.1   Paper I: Sander, M., Bengtsson, L., Holmquist, B., Wohlfarth, B. and Cato, I., 2002: The relationship between annual varve thickness and maximum annual discharge (1909–1950), Journal of Hydrology vol. 263, pp. 23–35.

This paper concentrates on deriving robust paleo-discharge from the thickness variation seen in the varve series in Ångermanälven, central Sweden. First, 11 varve series were amalgamated into a geometric mean. The mean varve thickness correlates well to

maximum daily annual discharge measured at Sollefteå hydrological station during the period 1909–1971 A.D. The correlation coefficient (r =0.87) of the raw data is based on a linear fit between the two data sets. However, a visual curved trend suggested that a power or logarithmic model would better describe the relationship. By rebooting the data, randomly extracting a group of data points and calculating correlation coefficients for linear, logarithmic and power models it was shown that the linear model yielded asymmetric populations of linear regressions, while the logarithmic and the power model yielded symmetrical results.

The three different models (power, logarithmic and linear) were further scrutinized by investigation of the distribution of three reconstructed discharge series derived from them, which were calculated by a least squares regression analysis of the 1909–1971 A.D. data. This calculation was made by using the distribution of the observed discharge as a scale for the distribution of reconstructed discharge. Since the reconstruction is designed to produce maximum daily annual discharge, i.e. an extreme event, it was reasonable to view the data as a series of extreme events and the Gumbel distribution.

Two exceptionally thick varves in the 2000 year long varve series are present: 465 and 658 A.D., c. 15 and 30 cm thick respectively. These two varves should be representatives of the 2000 and the 1000 year floods, respectively, and their heights correspond to what is expected based on a scaling of the observed maximum daily annual discharge series. The linear model derived a very high discharge for the 658 A.D. event, corresponding to the 60,0000,000-year return

flood. To put this return time in a geological perspective, the flood of 658 A.D. would have been the most powerful flood in Ångermanland since the end of the Cretaceous period and greater than any flow to be expected during the last deglaciation, which is unlikely. The logarithmic model yielded a result for the 658 A.D. event that was comparable to that of the observed series (3500 $m^3 s^{-1}$). The power model yielded a result (4600 $m^3 s^{-1}$), in between those of the linear and logarithmic models and was regarded as the best performing model of the three. This conclusion can also be supported by conceptual considerations of flow and transport. Water flows with a velocity (V), which is proportional to discharge (Q). The transport of particles is related to the area acted upon and is thus proportional to V^2. Combined transportation is proportional to V^3. Finally the transported sediment is proportional to the amount of sediment eventually deposited, i.e., to varve thickness. Thus, before considering more complex models involving flow type, grain size distribution, river geometry and hydro-dynamics it can be expected that varve thickness is related to discharge through a power function with an exponent close to a value of 3.

The maximum daily annual discharge series derived from the power model was divided into 50 successive 40-year periods and the maxima for each period extracted. The distribution of this data set should be comparable to that of the observed maximum discharge if scaled with the appropriate parameter. However, the 2000-year period deviated from the scaling of the observed maximum daily annual discharge at intermediate values. A discharge plateau occurs at 3500 $m^3 s^{-1}$, which indicates that natural discharge may not easily exceed this threshold. On the other hand, the extreme events at 492 and 658 A.D. lie within the anticipated range, as do lower discharges (< 3000 $m^3 s^{-1}$).

The result of Paper I is an optimal reconstruction of maximum daily annual discharge from Ångermanälven for the last 2000 years. The variance in reconstructed discharge can be explained by natural fluvial variability. No slumps, earthquakes (Mörner, 1996) and landslides are needed for justification of the extreme events.

5.2 Paper II: Sander, M., Holmquist, B., Wohlfarth, B. and Cato. I., 2002: A 2000 year long record of snowmelt flood derived from a clastic varved sequence and its relation to snow pack changes, in central Sweden.

The dependence of varve thickness on discharge has been known ever since G. De Geer measured the first varves in the late 19th century, although the precise relationship has never been established. As already demonstrated, the maximum daily annual discharge was isolated as the major governor of varve thickness (Paper I, section 5.2). Maximum daily annual discharge normally occurs during the SMF in May or June, and in principle varve thickness variation can be linked to snow accumulation during the winter. Within the catchment of Ångermanälven 9 meteorological stations have a precipitation record and two stations outside the catchment have recorded long precipitation series, which potentially contribute to the variation in SMF. However, because precipitation is unevenly distributed and melt pulses occur at different time in different places, the variability recorded in the SMF at Sollefteå and hence in the varve series is likely to be a patchwork of melt water pulses from regional snow packs.

Accumulated observed Winter Precipitation (AWP) for the 11 stations (October to March) gave a reasonable estimate of the mass of the snow pack that contributes to the SMF flood in May or June. The 11 stations are distributed in four regions: mountain area (3), inland out (2), inland in (5) and coastal area (1). If the snow pack contributes to the SMF the variability of AWP should co-vary with the observed SMF and be reflected in the varve thickness. The data from two stations did not co-vary with the SMF and varve thickness and were excluded. The remaining series, which did covary with SMF, were averaged and stacked to form a single series (1920–1950 A.D.), representing Average Accumulated Winter Precipitation (AAWP). This procedure ensured that the variability in the local snow pack was accounted for in the AAWP. The AAWP was found to be significantly correlated to observed SMF and reconstructed SMF. Thus, the AAWP series was found to explain ~40% of the variance in SMF.

Given the above explanation it was reasonable to assume that some of the variation in the 2000-year long series of varve thickness was related to changes in AAWP changes. Although a reasonably strong correlation, it is not justified to produce an annual AAWP record. However, it is strong enough to associate the long trend of varve thickness to trends in AAWP. Reconstructed SMF shows centennial variability, which is comparable to the Late Holocene climate succession for at least North Europe. Low SMF's are persistent during the Roman Warm Period (RWP) 300 B.C.–400 A.D., followed by high SMF's during the Dark Ages Cold Period (DACP) 400-600 A.D., declining into a SMF minima in Medieval Warm Period (MWP) 900–1300 A.D., thereafter a maximum during the Little Ice Age (LIA) 1450–1900 A.D., culminating during the late half of the 19th century, then a short decline which is

associated with the Contemporary Warm Period (CWP), 1900–1950 A.D.

Comparing the Late Holocene reconstructed SMF with the GISP2 δ^{18}O curve revealed an interesting phenomenon. Based on the (winter) temperature seesaw pattern across the North Atlantic, an anti-phase relationship would be expected. The analysis indicates that this "seesaw" was present from 1700 A.D. until present. However, between 800 and 1700 A.D. the two proxies are in-phase, which indicates the absence of any North Atlantic Oscillation (NAO) influence on the varve thickness during this period.

As it has been suggested that a warming trend will strengthen the hydrological cycle and increase total annual precipitation the effect of a lower AAWP produced by shorter winters could be counteracted by more intense periods of solid winter precipitation. On the other hand, a cooling caused by the southwards movement of the polar front could lead to an artic desert scenario with extremely low precipitation. Thus, although conceptually simple, the effect of climate change is a delicate case of equilibrium best resolved in numerical models. In Ångermanland a warming may increase annual precipitation, but the solid precipitation accumulation period will shorten. The combined effect of warming is a lower SMF and *visa versa* for a cooling trend. Paper II presents one of the few winter precipitation proxy series beyond the instrumental series.

5.3 Paper III: Sander, M., Holmquist, B., Snowball, I. and Cato, I. 2002: Periodicities in the varved record of Ångermanälven; – Evidence for solar and atmospheric forcing?

The presence of frequencies in climate and climate proxies has been studied for more than a century, as curious phenomena of nature, and for long range forecasting. Paper III investigates the frequencies embedded in the younger part of the STS in the light of renewed attention on possible solar forcing.

The 2000 year long geometric mean varve thickness record was analysed by Fourier analysis (by periodogram) and Morlet-wavelet analysis. Although both analysis techniques detect frequencies in time-series, they differ widely in statistical method. The Fourier analysis essentially checks for frequencies at a range of stationary values, in this case 100 fixed frequencies from 2–N year band, while the Morlet wavelet handles the non-stationary behaviour of frequency bands through time. Thus, if a natural data set holds a non-stationary frequency in the band 10–12 years, which may even be absent at times, there is high probability that Fourier analysis will not detect

it. In principle (but not always in practice) it should be detected by a Morlet-wavelet analysis.

A Fourier analysis of the 2000-year long record revealed a number of significant frequencies and indicated the presence of an insignificant c. 10 year cycle. Due to the mathematical design of the Fourier analysis by periodogram the insignificance of the c. 10 year cycle could be due to: (i) sporadic absence of a c. 10 year frequency, (ii) spontaneous phase shifts, i.e., that the phase do not make up a continuous wave, (iii) the non-stationarity of the c. 10 years frequency. By dividing the dataset into time segments some of the problems associated with changing frequencies can be avoided and this division was done to (i) isolate the periods when the 10-year frequency was absent, (ii) isolate periods of different phases, (iii) isolate stationary frequencies in separate segments.

The 2000-year long record was divided into 6 segments, four successive 500-year segments and two 1000-year segments. Significant frequencies within the 9–13 year band were detected in all these subsegments, but at distinctly discrete frequencies. These subtle changes in frequency during different periods explained why the 10-year cycle was not detected when the 2000-year long record was treated as one segment. The total of seven Fourier analyse revealed strong short sub-decadal frequency (2–5 year) variability throughout the varve series, a persistent but non-stationary (decadal) 9–13 year frequency and centennial variability, which was supported by the Morlet wavelet analysis.

The inter-decadal variability could be tentatively associated to variability of the NAO (the pressure gradient between the Azores high and the Icelandic low), which has some control of the winter precipitation pattern over central Sweden. However, the association was only based on the recognition of frequencies. Additional analysis showed that AAWP also held frequencies in the same band. Thus, it seemed reasonable to associate the fast frequency band to variability in ocean/atmosphere coupling in the North Atlantic.

The decadal frequency (9–13 year) is identical to the frequency band observed in the sunspot (number) series. A signal to noise analysis between a 7-year running mean of the varve thickness and the sunspot (number) series (SNR) indicated maximal coherency at 1-year lag, with a surprising varve lead. However, the increase in SNR by assuming one year lag is negligible compared to a zero lag. In addition, the annual sunspot series are calculated from monthly values based on a calendar year, whereas varve thickness must be related to a hydrological year (SMF to SMF). Thus, there is room for reasonable mathematical adjustment that will synchronise the

two proxies, i.e. zero time lag. Calculation of the correlation coefficient (r) showed that varve thickness variability and the sunspots number record are only weakly correlated (r=–0.15 and t=2.16).

The weak correlation is negative, i.e. increased solar activity is correlated to thin varves and *visa versa*. This correlation is in agreement with the result of Paper II where LIA varves were found to be thick and MWP varves to be thin. During the same respective periods a low (Maunder minima) and a high of sunspot were persistent. Thus, the varve series holds a non-stationary c. 10-year cycle (Schwabe cycle), which during the observed period is in anti-phase with the observed sunspot number. Likely solar variability on decadal timescales forces varve thickness variations. Naturally, it is not the observed number of sunspots that controls varve thickness, but the wide range of associated parameters that are affected by the sunspot cycle, such as variation in irradiance, particle flux and the deflection of cosmic radiation.

A centennial cycle is detected in the 2000-year long series. The wavelet analysis and a 51-year running mean suggest that no centennial variability is present in the varve record between 0 and 600 A.D. Centennial variability is probably related to the Suess cycle. The reason for its absence during the 0–600 A.D. section of the varve series may be due to an internal river system threshold, i.e. that discharge of certain heights are not easily trespassed due to catchment configuration and melt water generation rates. Varve thickness was relatively thick during the DACP and it is hypothesized that the variability forced by the Suess cycle is diminished during such periods. As shown in Paper II the maximum discharge distribution possesses an internal threshold at around 3600 m^3s^{-1}. Significant external forcing is required to pass this threshold and, therefore, weaker forcing of the discharge at this threshold level will not be detected in discharge records, or the varve series. Finally, a weak millennial waveform was observed in the Late Holocene climate succession. A significant part of the 2000-year varve record could be explained by the superposition of 4 frequencies, (i) a frequency in the 2–5 year band, (ii) a c. 10 year frequency, (iii) a centennial cycle and (iv) the more speculative millennial scale cycle. These are associated with the high-frequency ocean/atmosphere variability, the solar Schwabe cycle, the solar Suess cycle and ocean/atmosphere vacillation connected to the Bond cycle, respectively (Bond *et al.*, 1997; Damon *et al.*, 1998).

6.0 The relationship between reconstructed snowmelt flood and climate proxies

In most fields of science extensive correlation analysis is not considered good practice, primarily because significant correlations can arise by chance. Correlations can be found between non-related series and, from a conservative viewpoint, statistics should be used to describe an already proven relationship. However, in geology statistics are increasingly being used to detect potentially casual links between forcing factors and the archives of environmental response (e.g. Wohlfarth *et al.*, 1998). The present author has conducted hundreds of cross-correlation analyses, each of them producing a multitude of correlation coefficients and SNR's. Of these 5% can be expected to be significant by chance. The geometric mean varve series has been correlated to a wide selection of annually resolved paleo-climatic records and meteorological data in the vicinity of Ångermanland and in the North Atlantic region.

Normally before embarking on any statistical analysis a null hypothesis is formulated. According to Popper (2002) a hypothesis should be formulated in such a way that falsification is much more easily obtained than verification. Indeed in a strict Popperian sense, nothing is certain (proved), only not yet falsified. It has been claimed that the progress of science may be more rapid if non-Popperian philosophies are followed.

Due to the retrospective nature of geology it is impossible to conduct real-time experiments designed to reject hypotheses. Indeed, Quaternary geology is almost devoid of any falsification experiments. Instead the scientific community is occupied with pattern recognitions, e.g. the signature of glacial-interglacial climate variability registered in different natural archives, e.g. Björck *et al.* (1996). In this chapter the co-variation between the SMF and a number of other proxies is tested. It is, therefore, essentially accepted that causal co-variability exists between varve thickness and the respective proxy dealt with, otherwise it would be pointless to conduct the analysis. A null hypothesis approach is rejected; the basic question asked is not if there is co-variation, but how strong is it and is there a reasonable physical explanation for the found co-variation?

The constant hypothesis herein is that proxies which can be positively related to annual or winter temperature in the near vicinity of Ångermanälven are negatively related to SMF and, thus, varve thickness. In addition, it is hypothesized that proxies that are positively related to summer/spring temperature are positively correlated to SMF. In other words, cold

winters and low annual temperatures increase SMF and a high rate of temperature increase during the spring and/or summer months increases SMF. This hypothesis is based on the output of numerical models e.g. (Gleick, 1989) and the result obtained from the recognition of a typical late Holocene climate succession in the varve thickness series (Paper II).

The majority of the analyses referred to are presented in App. V. Due to space restrictions, NAO observed vs. SMF is omitted. Only cross-correlation figures are shown in App. V, although the entire three-step analysis is described in the section 4.1.

Note that reconstructed SMF, observed SMF and varve thickness are used interchangeable in context with the different external climate sensitive proxies. This is mainly due to the limited temporal range of the instrumental data series, which began in 1909 A.D., and does not allow for comparison further backwards in time. Although varve thickness forms the basis of the raw data set, the causal physical link requires that these data reflect discharge variations. As has been shown (Paper I) the difference between the three SMF parameters is negligible as varve thickness is related to SMF reconstructed through a power equation derived from the relationship between observed SMF and varve thickness. All three proxies are causally related to each other and share variability.

6.1 Temperature vs. snowmelt flood

Temperature variation is expected to influence varve thickness, not least because the spring temperature rise causes snowmelt. Temperature may also influence precipitation, as a warmer atmosphere potentially contains more water vapour than a cooler one. Therefore, a temperature forcing may be present both during the accumulation- and the melt- period. Thus, it is expected that some variation in SMF can be explained by variation in a suitable temperature record. Temperature during accumulation is expected to be inversely correlated to SMF, temperature during melt is expected to be positively correlated to SMF.

Temperature records have been obtained from within the Ångermanälven catchment (i), in the near vicinity (ii) and outside the catchment (iii): (i) Junsele, Forse, Gäddede, (ii) Stensele, Härnösand (iii) Stockholm and Uppsala. (Table 1 and Fig. 1) The records within the catchment are short (max 10 years), those in the near vicinity are of intermediate (140 years) range and those of Stockholm and Uppsala among the longest in Europe (Table 1). Normally temperature variation signals are regional, e.g. the Uppsala and Stockholm series are virtually iden-

tical (Moberg, 1996) and thus the year-to-year variation is expected to be reproduced in different series. This co-variation facilitates the use of the long series of Stockholm and Uppsala, which otherwise could be argued to be located too far from the watershed.

The temperature series were checked for monthly and seasonal co-variation with and SMF. Since the melt of the accumulated snow pack produces the SMF no relationship should exist between SMF and the temperature of the precedent January–May period. However, the temperature of the late autumn and early winter at the end of one calendar year can, hypothetically, influence the subsequent SMF.

Weak correlations, which contradicted the above hypotheses, were found between temperature records and SMF reconstructed (Table 1 and App. V). The records of monthly temperature within the catchment and in it's near vicinity generally share positive variation with the SMF reconstructed in February or March. However, the sign of the correlation changes from positive inside to negative outside the catchment, which indicates that higher temperature forces increased SMF within the catchment, while higher temperatures outside the catchment decreased SMF. For the Stockholm and Uppsala data the results are elusive, negative correlations were found in three instances, allowing for a one-year time lag (SMF leading). However, the seasons and months associated with the time lag are not-consistent with the observed hydrological cycle.

The theoretical forcing of SMF by temperature cannot be proved by the statistical approach. The positive correlations found between winter temperature within the catchment and SMF contradict the anticipated relationship. The few spring/summer temperature series that share significant amount of variance with SMF also contradicts the anticipated relationship (Table 1). The effect of temperature is difficult to predict due to the its complex influence on the snow pack, soil and groundwater. Although the spring temperature rise generates melt water, a deep snow pack and underlying soil (if not frozen) can absorb water. Thus, the true temperature influence is likely to be via the rate at which the saturated snow pack melts. This temperature rise rate is hardly captured by any of the monthly or seasonal temperature series presented here.

6.2 Tree-rings vs. snowmelt flood

Theoretically, the width of tree-rings within the catchment may be correlated to varve thickness, since tree-ring width is a reflection of summer temperature and autumn precipitation (Linderson, 2000). Tree-ring series from two regions in Sweden were com-

Table 1. Correlation table of temperature vs. SMF reconstructed

	Forse 1904–1950 A.D.	Junsele 1909–1950 A.D.	Gäddede 1906–1950 A.D.	Härnösand 1859–1950 A.D.	Sensele 1861–1950 A.D.	Stockholm 1756–1950 A.D.	Uppsala 1722–1950 A.D.
Jan	*	*	*	*	*	*	*
Feb	*	*	0.31	*	0.24	*	*
Mar	0.41	0.36	0.38	*	*	*	-0.19#
Apr	*	*	*	*	*	*	*
May	*	*	*	*	-0.22	*	*
June	*	*	*	-0.27	*	*	*
July	*	*	*	*	*	-0.17	*
Aug	*	*	*	*	*	*	*
Sep	*	*	*	*	*	*	*
Oct	*	*	*	*	*	*	*
Nov	*	*	*	*	*	*	*
Dec	*	*	*	*	*	*	*
Seasonal							
MAM	0.30	*	*	*	*	-0.20#	*
JJA	*	*	*	*	*	*	*
SON	*	*	*	*	*	*	*
DJF	*	*	*	*	*	*	*

Table 1. Correlation table of temperature vs. snowmelt flood reconstructed. Significant but enigmatic positive and negative correlation coefficients were found. * marks insignificant correlation coefficients, (confidence level =95 %), numerical value not shown. The data series were tested for lead and lack. Reasonable time-lack is summer-winter temperature influence the proceeding snow accumulation and varve thickness. # mark significant correlation with temperature leading one year.

pared to the SMF, (i) five series from Ångermanland and (ii) the Torneträsk series (Fig. 1). The Ångermanälven series are short compared to the Torneträsk series (Table 2), and were correlated to temperature and precipitation data sets from nearby meteorological stations (Linderson, 2000). The main governor of the ring width is summer temperature, although an autumn precipitation signal is also present. The five series were measured in the three landscape zones. Two in the mountain area near Gäddede, two in the inland area near Junsele and one in the coastal zone near Multrå (Fig. 1). Thus, there is a good spatial coverage of tree ring data in the catchment, particularly with respect to precipitation variation (chapter 3.4).

Although tree-ring series from Ångermanland have been specifically correlated to summer temperature (Linderson, 2000), that signal could be a reflection of annual temperature variation rather than a signal of increased summer temperature on the background of invariant autumn, winter and spring temperature i.e. increasing seasonally. Two hypothetical relationships could give rise to co-variability between tree-ring widths and SMF; (i) that the temperature signal in the tree-rings is annual and influences snow accumulation, so that ring width would be negatively correlated to SMF, (ii) that the temperature signal is related to the spring temperature rise that causes snow melt, so that ring width would be positively correlated to SMF.

The conifer series come from Ångermanland (Linderson, 2000). Five series were constructed from living trees, two *Picea* and three *Pinus* series (Table 2). Three components were measured, early wood, late wood and total thicknesses (due to measurement tech-

Table 2. Correlation table between tree–ring series from Ångermanälven and Torneträsk vs. Snowmelt flood reconstructed.

Tree–ring series	Species	Internal reference point		Period covered
Långbroberget	*Pinus*	1, 0209 (Linderson, 2000)		1722–1950 A.D.
Junsele	*Pinus*	2, 0509 (Linderson, 2000)		1838–1950 A.D.
Ruskhöjden	*Picea*	3, 1609 (Linderson, 2000)		1723–1950 A.D.
Storvattenet	*Pinus*	4, 0909 (Linderson, 2000)		1854–1950 A.D.
Hillsandhöjden	*Picea*	5, 1909 (Linderson, 2000)		1827–1950 A.D.
Tornaträsk	*Pinus*			436–1950 A.D.
Junsele		**r**	**t**	
Early wood		0.02	0.16*	
Late wood		0.05	0.52*	
Total ring		0.02	0.18*	
Storvattenet		**r**	**t**	
Early wood		0.10	0.95*	
Late wood		–0.06	–0.59*	
Total ring		0.07	0.65*	
Långbroberget		**r**	**t**	
Early wood		–0.19	–2.85	
Late wood		–0.17	–2.65	
Total ring		–0.19	–2.86	
Ruskhöjden		**r**	**t**	
Early wood		–0.09	–1.33*	
Late wood		–0.10	–1.54*	
Total ring		–0.09	–1.42*	
Hillsandhöjden		**r**	**t**	
Early wood		–0.06	–0.65*	
Late wood		–0.10	–1.00*	
Total ring		–0.06	–0.65*	
Tornaträsk		0.10	4.01	

Table 2. Correlation table between tree–rings and reconstructed SMF, r = correlation coefficient, t = student t–test. * insignificant correlation

niques the total thickness does not always correspond exactly to the sum of early and late wood). Early wood could be related to the SMF of the same year and the late wood to the following year SMF. The late wood layer is thinner than that of the early wood layer and the total ring width is strongly influenced by the thickness of the early wood. The three tree-ring components were all compared to SMF by cross-correlation. Juvenile wood data were removed before analysis.

Cross-correlation results contradicted the hypotheses. Significant correlations were found, but these suggested a time lag of 1 year. This lag could be due to incorrect varve/tree-ring chronologies, but that is unlikely. A significant correlation with zero time lag was found between reconstructed SMF and the Långbroberget series ring width, which originates from Multrå (Fig. 1). However, as shown in Paper II the instrumental data obtained from Multrå (precipitation) and the coastal region (temperature) are consistently uncorrelated to varve thickness and SMF.

In the other tree-ring series no significant correlations to SMF were found with zero time lag or even allowing for a one year lead in case of the precipitation influence on late wood. The Långbroberget tree-ring series shares variability with the two *Picea* series, but these series are not significantly correlated to the reconstructed SMF. The negative correlation (Table 2) suggests that thicker tree-rings (warmer summers) are related to thinner varves and *visa versa*, a confirmation of the expected relationship, if the summer temperature is anticipated to be an effect of generally increased annual temperature.

The total ring width of the Torneträsk series is positively correlated to the reconstructed SMF series (r=0.10, t=4.01), although the correlation is confined to the long-term trend (centennial to millennial). The correlation is probably due to the typical Late Holocene climate succession or perhaps an even longer waveform. However, it is well known that long-term (millennial) climatic trends seen in several other proxy climate records have not been detected in dendrochronological series. Cross-correlation shows that the SNR peaks at zero time lag. It should be noted, however, that a significant correlation is obtained across a wide range of lag, which indicates that the correlation is present in the centennial-millennial trend (App. V). The correlation is weak (r=0.10) but gains significance due to the length of the record. The positive sign of the correlation contradicts the expected relationship between SMF and tree-ring width. It is acknowledged that thicker rings result from a warmer growth period and should, therefore, correspond to thinner varves, if it is assumed that increased summer temperatures are also an expression of increased annual temperatures. The

positive sign of correlation does not support the annual temperature increase inferred from tree-rings.

In short, the correlation analysis between tree-rings series and SMF was futile. No convincing correlation was found, even if a one-year lag in the majority of the series was allowed for. One tree-ring series from Långbroberget was found to be significantly correlated, albeit weakly, with the SMF. However, the climate of the coastal province from which it originates has little influence on the SMF and thus the varve thickness. The correlation to Torneträsk is confined to the long centennial-millennial trend and the sign of the correlation is opposite to that expected.

6.3 Geostrophic wind, Vorticity, North Atlantic Oscillation and North Atlantic Oscillation reconstructions vs. snowmelt flood

Lamb is a classification scheme, which has been applied to Sweden (Chen, 2000). In a similar fashion to NAO, it uses atmosphere pressure to derive different sets of atmosphere parameters i.e. zonal flow, meridional flow, geostrophic wind and vorticity. In contrast to the NAO, which is an index of North Atlantic baroclinic gradient between two points, the Lamb classification is local with 16 pressure stations positioned in and around Sweden in a grid system. The local Lamb classification potentially surpasses the NAO as an explanatory factor for any climate parameter measured or reconstructed in Ångermanland. Six indices can be extracted from the Lamb, although here only geostrophic wind (V) and vorticity (ζ) are compared to SMF. Deliang Chen provided the Lamb classification indices (http://www.gvc.gu.se/ngeo/deliang/deliang.htm#data)

The NAO is a frequently cited expression of decadal climate variability, originating from differences in the pressure gradient between the Azores high and the Icelandic low (Hurrel, 1995). The NAO has been shown to control a variety of climate parameters, especially winter temperature and precipitation and thus it may also influence the height of the SMF in River Ångermanälven. However, the instrumental NAO is only based on two geographic points and the gradient between them. If the centres of the high and low pressure cells associated with these points are not positioned directly over the stations the gradient will deviate from reality. The instrumental NAO was downloaded from (http://www.ngdc.noaa.gov/paleo/recons.html).

A winter NAO reconstruction was also compared to SMF, although such reconstructions should be approached with extreme caution (Schmutz *et al.*,

2000). The Cook *et al.*, (1997) data are based on tree-ring width and as such have annual resolution. Although, the tree growth period is a summer proxy the authors claim that a winter NAO signal can be derived. NAO index data were obtained from (http://www.ngdc.noaa.gov/paleo/recons.html).

In the Lamb classification the geostrophic wind (Fig. 7), the combined vector of zonal and meridioinal flow are calculated on a monthly basis, which enabled a comparison (cross-correlation) to monthly discharge variation as observed at Sollefteå (1909–1950). The SNR is very high (negative) at zero time lag, but displayed an oscillatory behaviour as the cross-correlation progressed in incremental steps (App. V). The correlation is confined to the 12 data point band (equivalent to one year). The oscillatory behaviour is due to the strong seasonality in both series; discharge rises to a maximum during snowmelt, which is superimposed on a moderate background flow for most of the year (Fig. 2). The geostrophic wind also shows a similar seasonality, numerically high during winter and low during summer, with a dominant frequency around 12 months, i.e. one year. Progressively moving the records one-year in either direction (lead or lag) brings the seasons into phase. It is problematic to claim that the geostrophic wind forces observed monthly discharge. If the geostrophic wind exerts a dominant influence on discharge then it should be possible to show that numerical changes in an extracted annual mean of the geostrophic wind are transferred into the SMF.

To relate a part of the monthly geostrophic wind values to annual SMF involves an "arbitrary" choice of the monthly geostrophic winds that can influence SMF. According to the three papers and the correlation between AAWP and SMF it is likely that any relationship between the geostrophic wind and varve thickness arises during the winter months. A mean of winter geostrophic wind was calculated (October to May) and compared to reconstructed SMF (1874–1950 A.D.) with the results of r=0.10 and and t=0.83. The winter/early-spring mean of geostrophic wind is, therefore, not significantly correlated to reconstructed SMF.

Extreme precipitation events may be dependent upon extreme atmospheric situations and to test this hypothesis the annual maximum and minimum of the geostrophic wind series were extracted and correlated to reconstructed SMF. The extreme maximum geostrophic wind was found to be weakly, but significantly correlated to reconstructed SMF (r=0.28, t=2.58). The series of minima geostrophic wind was not found to be correlated to SMF (r=0.07, t=0.65) (App. V).

The annual maximum in the geostrophic wind occurs during the winter period (Chen, 2000). Thus,

the correlation found may be significant and reveal a true physical link between the state of the atmosphere and SMF. However, the numerical handling is problematic, some maxima occur at the beginning of winter (end of calendar year) and must contribute to the SMF through AAWP in the next calendar year. Other maxima also occured in the same calendar year as SMF, but these took place before the SMF in the same calendar year. In order to sort out the geostrophic wind influence on SMF, the geostrophic wind data needs to be carefully scrutinised and the problem of finding composite records with recurrent time lag and synchronicity must be solved.

It is speculated that the geostrophic wind should share some variability with the precipitation series of the catchment. Since accumulated winter precipitation is the major governor of SMF, any tight relationship between precipitation and geostrophic wind will support the argument that the geostrophic wind influences SMF. Three stations were randomly selected: Östersund, Gäddede and Leipikvattenet (Fig. 1). Due to the strong seasonal variability in precipitation, the three meteorological stations and the geostrophic wind share variability in the annual cycle and all three stations are significantly correlated to the geostrophic wind. A peak in SNR is present at zero time lag in the cross-correlation between Leipikvattenet, Gäddede and the geostrophic wind (App. V). However, Östersund was found to be negatively correlated to SMF, while the two mountain series were positively correlated. Thus, it seems that the geostrophic wind acts in two opposite directions with respect to precipitation. The combined result of geostrophic wind on the catchment precipitation is ambiguous, as is its relation to SMF.

Lamb classification, the vorticity (Chen, 2000) (Fig. 7) is positively correlated to SMF for monthly data 1909–1950 A.D. (r=0.20 t=4.44). Following the result of the correlation exercise between geostrophic wind and SMF analysis a maxima and a minima series were extracted from the vorticity record and compared to reconstructed SMF (1873–1950 A.D.). The maxima series was found to be significantly and positively correlated to SMF (r=0.29 t=2.64). The minima series was found to be insignificantly correlated to SMF (r=0.19 t=1.67). The geostrophic wind argument applies; i.e. maxima in vorticity occur before and after the SMF depending on the maxima position in the calendar year with respect to the hydrological year.

Vorticity was found to be significantly correlated to precipitation on a monthly basis at the following meteorological stations: Leipikvattenet (r=0.12, t=3.66, 1914–1995 A.D.), Gäddede (r=0.27, t =8.51, 1915–1995 A.D.) and Östersund (r=0.49,
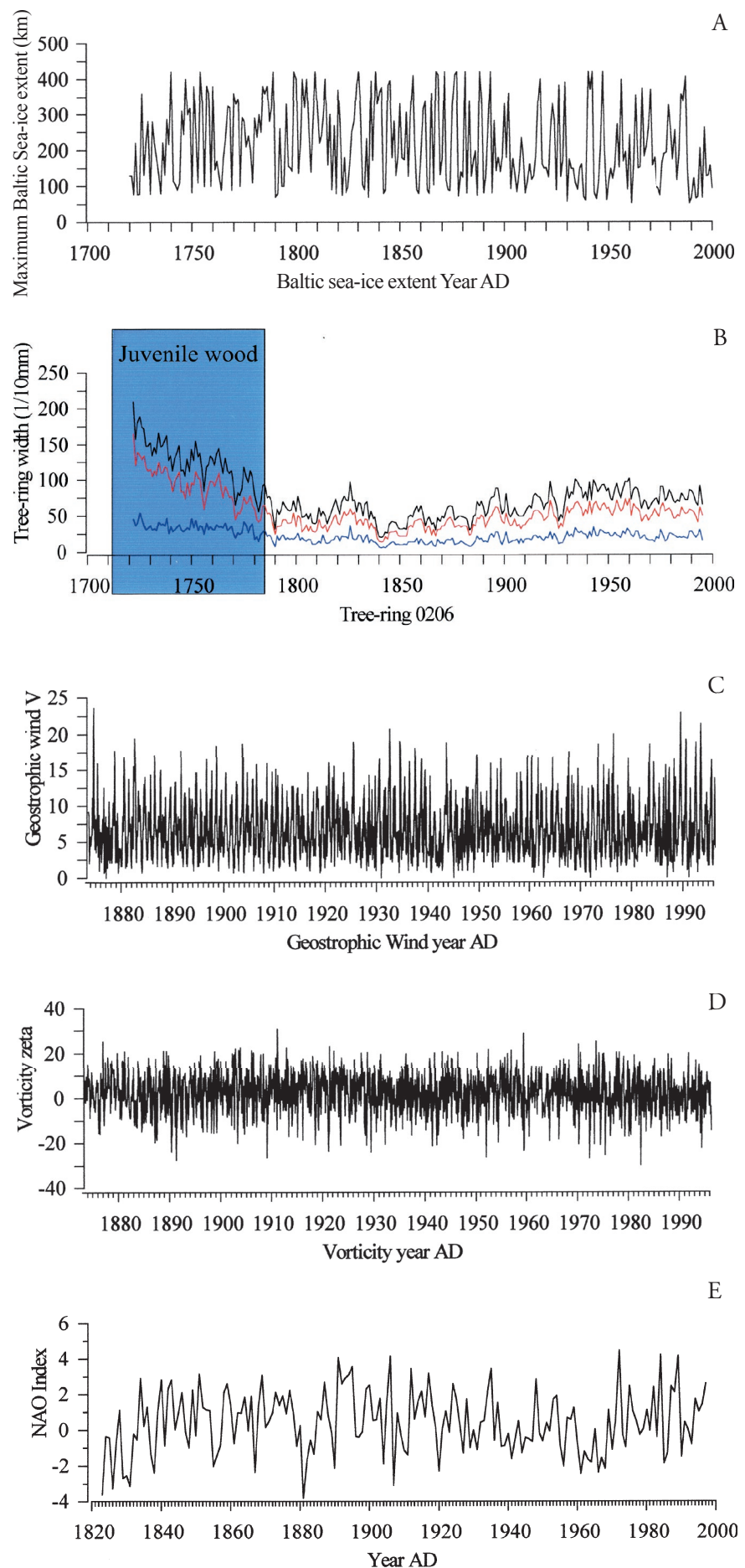
Fig. 7. Examples of proxies compared to the SMF. (A). Annual maximum Baltic sea-ice extent. (B). Tree-ring width, early- late wood and total ring width (blue, red and black), notice that the major part of each year's thickness is controlled to the early wood. Also notice the declining trend in the beginning of the record (juvenile wood). The trend is not a climate signal but an indication of rapid growth during the first decades of the tree's life span, consequently the juvenile wood was removed before analysis. (C), Geostrophic wind, i.e. the wind speed. (D). Vorticity, i.e. the circulation of the air-masses. (E), NAO, i.e. the barometrically gradient in the North Atlantic. Examples of temperature and precipitation are shown in Fig. 3 and 4.

t=16.45, 1874–1995 A.D.). In contrast to the geostrophic wind comparison all precipitation series were positively correlated to vorticity. Thus, vorticity has a landscape-independent influence on precipitation. The vorticity has two different modes, (i) positive and (ii) negative, depending on the direction of rotation i.e. cyclonic or anti-cyclonic. Positive vorticity is an expression of low pressure; negative vorticity is an expression of high pressure (Chen, 2000). The positive correlation to observed monthly precipitation for the three stations indicates that low-pressure forces increased precipitation and high-pressure forces decreased precipitation. Hence, the comparison between precipitation and vorticity strongly indicates that precipitation is governed by atmospheric circulation and that some shared variation should be expected between SMF and vorticity. However, this shared variability is hard to demonstrate due to noise in the SMF record and the problems concerning recurrent leads and lags of successive maxima and minima in the series.

Table 3. Correlation table between NAO and SMF reconstructed

	NAO obs. 1825–1950 A.D.	NAO Cook 1701–1950 A.D.
Monthly		
Jan	*	N/A
Feb	*	N/A
Mar	*	N/A
Apr	*	N/A
May	*	N/A
June	*	N/A
July	*	N/A
Aug	*	N/A
Sep	*	N/A
Oct	*	N/A
Nov	*	N/A
Dec	*	N/A
Seasonal		
MAM	*	N/A
JJA	*	N/A
SON	*	N/A
DJF	0.18	N/A
Annual	N/A	*

Table 3. Correlation table between NAO and snowmelt flood reconstructed. NAO obs. is the instrumental series of NAO. NAO Cook is a reconstruction, references given in text. * insignificant correlation, N/A (Not Available) Correlation not calculated due to the annual character of the NAO reconstruction. MAM: Marts, April, May, JJA: June, July, August, SON: September, October, November, DJF: December, January, February

The influence of NAO on European climate has been demonstrated both with respect to the instrumental meteorological record and to paleo-climatic archives e.g. (D'Arrigo *et al.*, 1993; Rodwell *et al.*, 1999). Since NAO handles the general situation of the atmosphere, which controls T and P, it is anticipated that the NAO variability exerts some influence on snow accumulation and its melting. A strong covariation between winter precipitation and NAO was demonstrated in Paper II and that the AAWP signal could be transmitted to SMF.

The sharing of variability between the NAO index and SMF is limited (Table 3), despite the strong influence of NAO on precipitation. The spring season (NAO) was found to be weakly and positively correlated to the SMF. Thus, although the NAO controls precipitation variability during winter, the noise added to the NAO signal during melt and river flow to the estuary erases NAO signal in the varve record.

Cook *et al.*, (1997) calculated the first (winter) NAO index reconstruction based on tree-ring records, six from eastern North America and four from Northwestern Europe. The reconstructed series spans the interval 1701–1980 A.D. and explains 41% of the variance in the NAO during the A.D. 1874–1980 calibration period. The reconstruction also captures the spectral properties of the observed NAO, suggesting that the oscillatory character of the NAO is a long-term feature of the North Atlantic climate system. (Cook *et al.*, 1997). The use of transatlantic tree-rings, which are likely to contain a large amount of summer temperature signal, may not produce a true winter NAO index. Since a tree-ring only has annual resolution the Cook *et al.*, (1998) NAO reconstruction is also annual and does not enable a month by month comparison. No correlation (SNR) with or without time lag was found between Cook *et al.*, (1997) NAO and reconstructed SMF (Table 3).

In summary, there is no conclusive evidence for a relationship between atmospheric circulation (index and indices) and SMF. The presence of NAO, geostrophic wind and vorticity signals are detected in instrumental winter precipitation series from Ångermanland and nearby meteorological stations, but they are not transferred through the melt water-varve formation pathway. Significantly noise must be added through unknown processes that are not directly related to the NAO, which obscures any potential NAO signal.

6.4   Global temperatures by Jones and Briffa vs. snowmelt flood

The reconstructed SMF of River Ångermanälven has been compared to one of the first "global" temperature reconstructions (Jones *et al.*, 1998) and a later temperature reconstruction based on tree-rings series (Briffa *et al.*, 1998a). The "Mann" curve (Mann *et al.*, 1999) was avoided due to its lack of variability besides the recent warming trend. Data was obtained from (http://www.ngdc.noaa.gov/paleo/recons.html). As with the other considered temperature proxies, it is hypothesised that global T is inversely correlated to SMF.

Jones global temperature (1000–1950 A.D.) has southern and northern hemispheric components and both are compared to SMF. Temperature sensitive paleoclimatic multi-proxy data from 17 sites worldwide were used to generate thousand year long records of temperature for both hemispheres. Proxy types include tree-rings, ice cores, corals, and historical documents (Jones *et al.*, 1998).

The northern hemisphere temperature reconstruction was insignificantly correlated to varve thickness when the raw data were analysed at zero time lag. Nevertheless, common variability is seen in the long trend. The SNR peaks with a lag of 36 years, which indicates that the best fit between unmodified data occurs at a considerable time lag. No known physical process is known that could explain such a time lag (App. V).

The shared variability in the long term and the time lag justified the calculation of filtered data series. A running median with a 51 year window was applied, which increased the overall SNR and correlation coefficient at zero time lag (r=–0.28, t=–9.10). The negative correlation is in accordance with the expected relationship; that a generally colder climate leads to thicker varves.

As a test of the reliability of a relationship between the global temperature composite and SMF, the southern hemisphere temperature signal was also compared to the SMF (App. V). Initial results indicated that the northern and southern hemisphere temperature reconstructions share variability in the long frequency band and are significantly and positively correlated to each other. Thus, based on the correlation between the north and south temperature series, it might be expected that the SMF would share variability with the southern hemisphere temperature reconstruction. The cross-correlation of raw data indicated a significant SNR at 10 years lag. Again, a 51-year running mean was applied to both temperature and SMF and the cross-correlation was repeated. The two averaged time-series are significantly correlated (r=–0.53, t=–19.20), which veri-

fies the predicted correlation between them. In fact, the correlation with southern hemisphere temperature signal correlation is more robust than with the northern hemisphere. This exercise shows that the interpretation of any correlation coefficient present between proxies whose physical relationship is not understood should be treated with extreme caution.

Briffa *et al.*'s (1998) northern hemisphere temperature reconstruction (1400–1950 A.D.), which is based on tree-ring data, was also compared to the reconstructed SMF. The data consist of three time-series representative of the Northern Hemisphere growing season temperatures for the period 1400–1994 A.D., derived from the means of 383 maximum latewood density chronologies from the northern Boreal forest (Briffa *et al.*, 1998a). Cross-correlation shows that the different temperature series are internally well correlated and that it is sufficient to correlate one global T series with the SMF (the NHD1). The SNR between raw data points peaks with a one year lag and the calculation of a running mean easily closes the one year gap. A mean with a 51-year window was applied and the cross-correlation repeated (r=0.43, t=11.02). The positive correlation contrasts with the previously established negative relationship between SMF and the long-term temperature trend (chapter 6.1, 6.2 and paper II). On the other hand, the positive correlation requires a mechanism that links the late wood temperature signal of the tree-rings to a subsequent winter temperature.

6.5   Maximum annual Baltic sea-ice extent vs. snowmelt flood

The annual maximum Baltic sea-ice extent (1720–1950 A.D.) is a measure of the maximum areal extent of ice in the Baltic Sea and the Skagerrak (Omstedt and Chen, 2001). A significant shift in the sea ice extent occurred in 1877, which was most likely the result of a change from a generally cold regime to one that has been warmer. It has been demonstrated that the Baltic sea-ice extent correlates well to the winter NAO signal, although the relationship seems nonstationary (Omstedt and Deliang, 2001). Thus, the sea-ice extent and the winter precipitation in Ångermanland are both correlated to the NAO winter index and it is hypothesised that SMF and the Baltic sea-ice extend share variability. The Annual maximum Baltic sea-ice extend data were provided by Anders Omstedt.

Since the annual maximum Baltic sea-ice extent is winter temperature dependent a positive correlation to SMF is expected. No time lag is expected between the annual maximum sea ice extent data and the SMF data because the annual maxima occur when

the sea ice extent reaches its most south-westerly position, which in all cases will be in the same calendar year as SMF in Ångermanland.

However, with zero time lag there is no significant correlation between the reconstructed SMF and the maximum extent of the Baltic sea-ice. This result should not be surprising, because NAO variability is only mirrored in the observed winter precipitation, not in the varve series. On the other hand, the cross-correlation analysis gives a small peak in SNR, with the sea-ice leading the SMF by one year (r=0.16, t=2.49).

If the time lag correlation is an expression of a real physical link between the two proxies, the sea ice extent of a specific year must influence the following winters' accumulation of snow in Ångermanland. However, since the total melting of both sea ice and AAWP effectively resets the system, such a physical link is difficult to imagine. Alternatively, a one year error in the either of the time scales could explain the discrepancy. Such an error is unlikely to exist because the sea ice extent is based on precisely dated observations and the varve series is tied to observed discharge and is composed of multiple well-correlated varve diagrams (Cato, 1987).

6.6   Volcanoes and snowmelt flood

Violent volcanic eruptions that emit aerosols into the atmosphere are known to influence the global mean annual temperature (Briffa *et al.*, 1998a; de Silva and Zielinski, 1998), and thus potentially also the snow accumulation and SMF in Ångermanland. It is anticipated that an abrupt cooling associated with volcano eruptions would lead to an increased SMF. In order for eruptions to have a global impact the eruption gases and aerosols need to enter the stratosphere and be resident for a significant time. Eruptions that reach the stratosphere are extremely powerful and/or located close to equator where the troposphere is relatively thin compared to higher latitudes.

Different approaches to identify volcanic forcing of climate are possible. By a non-parametric Kolmogorov-Smirnoff test it is possible to test whether two distributions are identical (i.e. the distribution of a sub-sample of volcano year SMF compared with the remaining SMF population). Years with significant volcano-forced climate signals were taken from the composite tree-ring data set (Briffa *et al.*, 1998a) and compared to the corresponding years in the SMF record. Of course, autumn and winter eruptions after the SMF in same calendar year would not influence the earlier SMF, and thus the effect will be on the SMF the following year.

The test revealed no difference between the distribution of effective volcanic forcing of climate in the reconstructed SMF record and the remaining data (1600–1950 A.D.). Statistically, there is no significant volcanic signal within the SMF series. In fact, there is a slight tendency for SMF's corresponding to years with a volcanic forcing signal to be of lower magnitude than surrounding years, which is inconsistent with the theoretical climate forcing of SMF, that colder climates generate higher SMF's (Paper II). The fact of apparent, but not significant, lower magnitude SMF's during volcanic impact years also raises some problems in comparison with the remaining data. The SMF series is dominated by relatively low magnitude SMF, with a few extreme high SMFs. This distribution means that a sample of lower magnitude SMF's would almost certainly be identical to the distribution of the parent population, with the result that it would be impossible to identify a volcanic forced climate signal in the reconstructed SMF.

6.7   ¹⁴C variations and snowmelt flood

Recently the relation between solar variability and climate has renewed recent attention, ranging from short decadal scales (Svensmark and Friis-Christensen, 1997) and to longer millennial scales (Bond *et al.*, 2001; Björck *et al.*, 2001). The theories on how solar variability forces Earth's climate system are briefly discussed in Paper III. One main theory postulates that increased solar radiation is meditated to the lower atmosphere via direct heating of the stratosphere (Haigh, 1996). Another theory suggests that cloud formation is positively related to the production of cosmogenic nuclides, which is modulated by the heliomagnetic field. Given the assumption of a relatively constant geomagnetic field intensity changes in solar activity will influence cloud formation (Svensmark and Friis-Christensen, 1997).

As a cosmogenic nuclide, ¹⁴C is produced in the upper atmosphere by high-energy protons entering the nucleus of atmospheric nitrogen atoms. The flux of protons and the production rate of ¹⁴C are dependent upon the state of the Heliomagnetic field, which shields the Earth from interstellar particle flux. Any variation in the Heliomagnetic field will influence the particle flux reaching Earth from Cosmos and force changes in the production of cosmogenic nuclides like ¹⁴C and ¹⁰Be (Raisbeck and Yiou, 1981; Stuiver and Groots, 1981).

¹⁴C has been measured in the long German tree-ring series for calibration of radiocarbon dates to an annual timescale (Stuiver *et al.*, 1998). This series have been compared to the varves of River Ångermanälven. It has been demonstrated that the Little Ice Age and the Medieval Warm Period are present in the geometric mean varve diagram from River
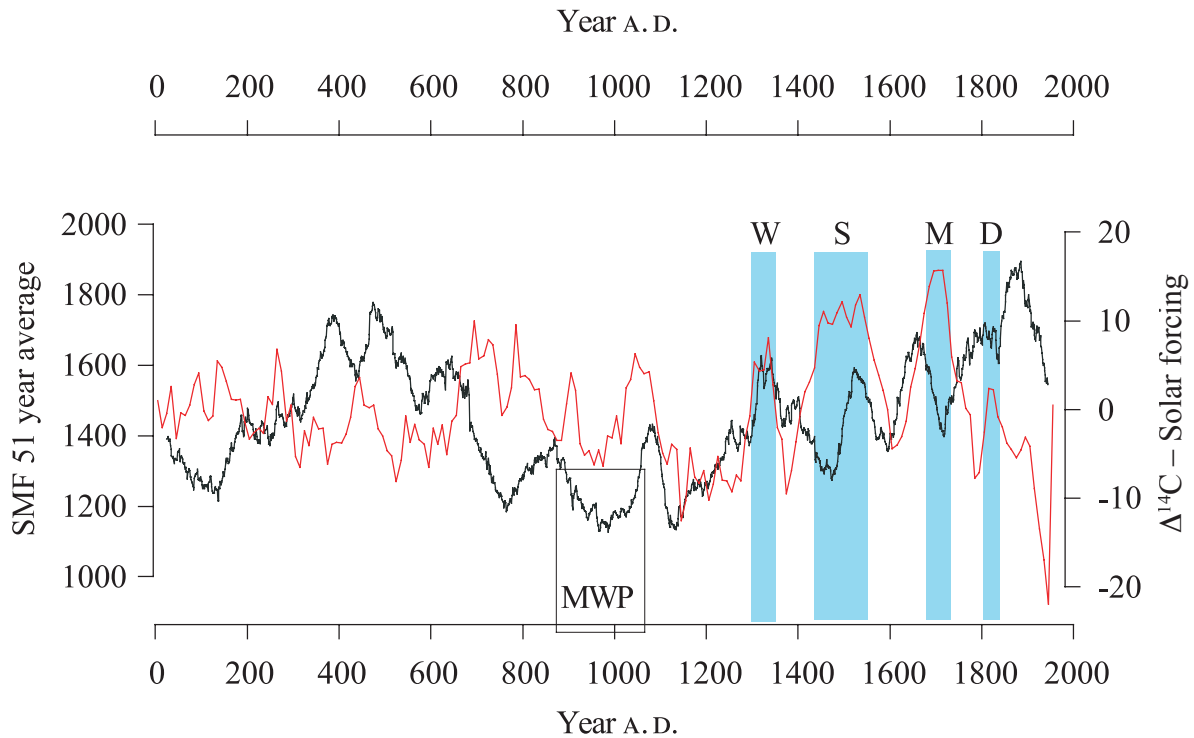
Fig. 8. *Skeleton plot of ΔC-14 (red) extracted from successive 10 tree-rings and SMF (black) reconstructed (51 year mean). M – Maunder minima, S – Spörer minima, D – Dalton minima, W – Wolf minima, MWP – Medieval Warm Period.*

Ångermanälven, both these periods are marked with a low respectively a high in the solar activity, thus potentially co-variation between the SMF and ^{14}C series may be present.

Due to the relatively long residence time of carbon in the atmosphere there is no point in extracting an annual ^{14}C record from tree-rings. Instead, a series of successive ten-year windows of ^{14}C content were extracted from the tree-ring series (Stuiver *et al.*, 1998) and this series is compared to the reconstructed SMF. The ten tree-ring sample size of ^{14}C does not allow for a direct cross-correlation analysis. The two records are compared in skeleton plots, as running mean with a 51 year window (Fig. 8). Based on previous arguments it is expected that low Δ^{14}C would correspond to thin varves. Periods of sunspot minima, such as the Maunder minima between 1650 and 1715 A.D. are contemporary with general thick varves and *visa versa*. Sunspot minima are accompanied by lower solar activity and during these times relatively more cosmic background radiation enters the Earths atmosphere and the production of ^{14}C increases.

Some variation is shared between the two series, especially in the younger part (1000 A.D. to present). However, the relationship is inconclusive, some peaks are positively correlated, while others are negatively correlated. The time spanning between 900 and 1700 A.D. is characterised by a negative rela-

tionship between the two proxies. This time span includes the MWP and the Wolf-Spörer minima. After 1700 A.D. and at the peak of the Maunder minima the apparent negative relationship disappears, with some indication that the relationship inverts to a positive one. Prior to 1000 A.D. there is no apparent correlation, with the exception of a positive relationship at c. 400 A.D.

6.8 Conclusive remarks of the forcing of SMF

In conclusion, it should be expected that the SMF and the varve thickness be driven by the combined effect of a plethora of different potential forcing factors. For example, if solar variability is one of the many factors forcing climate, there is still no reason to expect that the variability in a record of solar activity will be shared in any proxy-parameter (such as SMF) that reflects a complex climate system forced by several processes and subjected to positive and negative feedback mechanisms. A believable connection between Δ^{14}C and SMF is indicated for the MWP-Spörer period, but it may not be a sign of a true relationship, particularly when there is a mismatch within the remaining parts of the chronology.

The causal forcing of SMF is through winter precipitation and spring temperature rise. The winter precipitation predominance is well described where-

as the temperature signal remains elusive despite its obvious conceptual influence. For the remaining proxies tested in chapter 6 it has proved difficult to attribute any additional information on the forcing of the SMF. However, some influence on monthly precipitation and monthly discharge by atmospheric indices has been documented mainly for the winter period. These should be interpreted with care due to the strong seasonal character of both precipitation and discharge and the suggested forcing mechanism.

7.0   Revision of the post glacial period

Two issues will be addressed in this chapter, (i) new varve measurements from the River Ångermanälven, which are connected to the existing STS, and (ii) the cross-correlation analysis of varve connections published by Cato (1987 and 1998) (App. V). This analysis is motivated because a hiatus of c. 500 years has been suggested in the post glacial part of the STS.
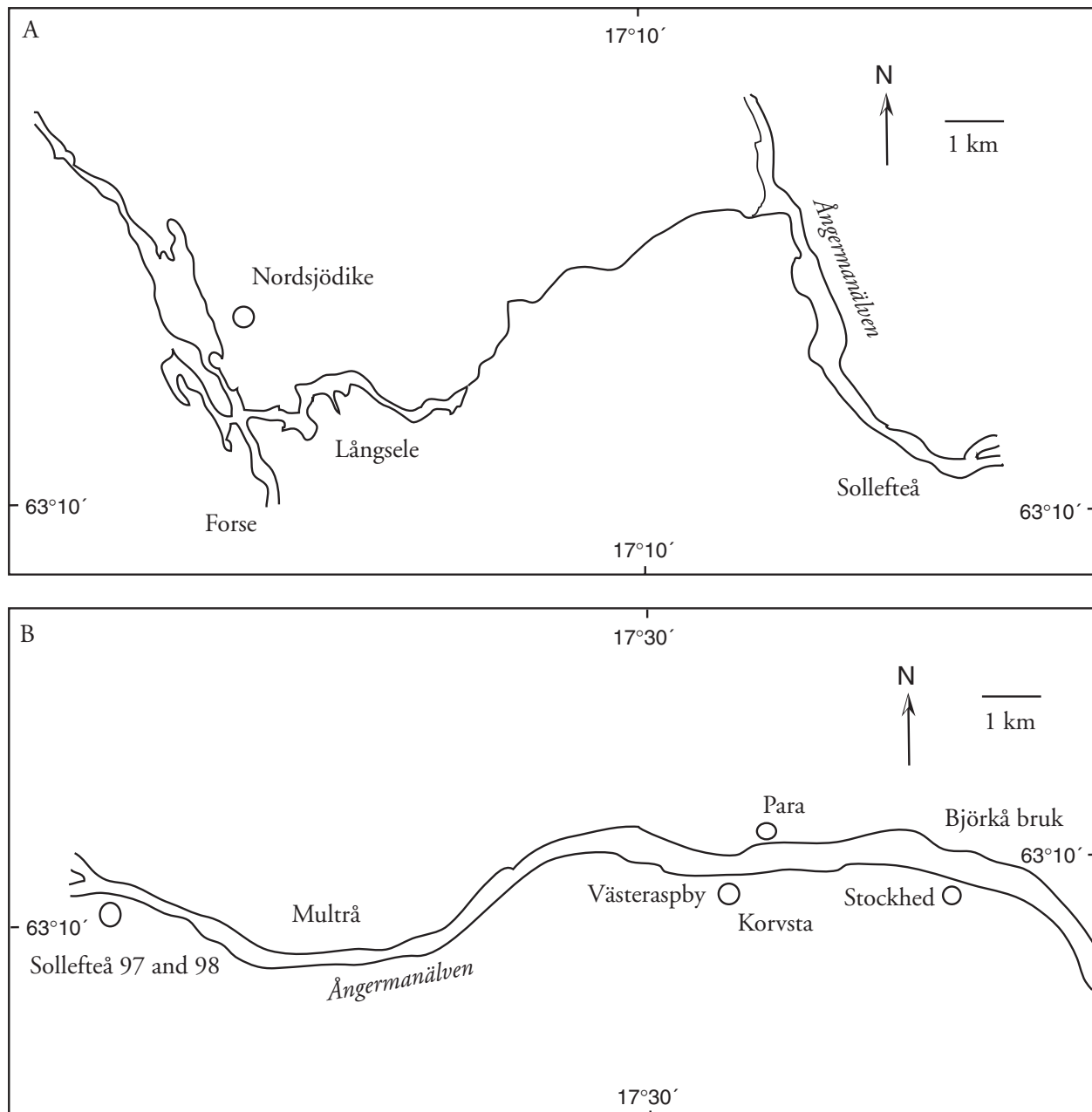
Fig. 9. *Position of the five new varve diagrams. Locations are marked with a circle. Nordsjödike located in the tributary of Faxälven are showed in Panel A, the remaining four series: Sollefteå-98, Västeraspby, Para and Stockhed located in Ångermanälven are showed in Panel B. Additional sites of R. Lidéns chronology are marked. Multrå, Korvsta and Björkå bruk. The two panel forms a continuous map, Panel A and Panel B west and east respectively.*

7.1 New varve diagrams

S. Björck and B. Wohlfarth measured five new varve series at a potentially erroneous section of the STS in 1998 (Fig. 9 and Table 4). A recently measured varve series, Sollefteå-97, has been connected to the STS (Wohlfarth *et al.*, 1997). The Sollefteå-98 series should form a continuation of Sollefteå-97. B. Wohlfarth provided the original paper strips with varves marked and the field notebook.

Björck and Wohlfarth's field-notebook describes that the topmost varve in Sollefteå-98 series corresponds to the –105 varve in the Sollefteå-97 series (measured in 1996) (Wohlfarth *et al.*, 1997) "Top of paper strip = –105 from 1996". The –105 varve is counted from oldest varve of the Sollefteå-97 varve diagram. At the depicted connection (–105) there is a peak in signal to noise ratio between Sollefteå-97 and Sollefteå-98 (App. V). Thus, the connection between the two series as described by B. Wohlfarth *et al.* (1997) is statistically significant. This confirmation extends the Sollefteå-97 time scale back to 4955 BP, compared to 4903 BP in the previous chronology (Table 4 and Fig. 10). However, it must be stressed that this connection is totally dependent upon the validity of the –105 connection. Excluding the –105 data point which is a relatively thick varve, also excludes any significant correlation (SNR) between Sollefteå-97 and Sollefteå-98.

The Para series is fairly long and displays high variability. A comparison to the two established series at Korvsta and Björkå Bruk (Cato, 1998) reveals that the numerical values of the varve thickness' are comparable to the delta proximal varves. Since Korvsta is located to the west of Para, it should be expected that the Para series in general are younger than Korvsta. Similarily, Björkå bruk is expected to be younger than Para and hence the Para section should fit to the younger part of Korvsta and to the older part of Björkå bruk. Since the Para series consists exclusively of proximal varves it is not possible in the first instance to connect the Para series to the Björkå bruk series, in which the contemporary varves will be distal delta varves.

A number of significant connections between the Para and Korvsta series are suggested by cross-correlation analysis. However, the procedure was very problematic. The best SNR is obtained by alignment of the thickest varves within each respective series. Unfortunately, this procedure involves the last and thickest varve of the Korvsta series, i.e. the presence of thick end varves control the outcome of the cross-correlation. The design of cross-correlation analysis makes it very sensitive to these thick varves and their removal leads to insignificant correlations. The chosen connection between Para and Korvsta marks a local positive peak in SNR within an area of generally low SNR and avoids the very thick varves in the end of the Korvsta series, but brings a number of other thick varves into alignment (Fig. 11).

Based on the connection between Para and Korvsta a connection to Björkå bruk is made, which supports the chronology made by (Cato, 1998). This connection brings the Björkå bruk and Para series into close agreement, supporting the connection to the Korvsta section and the STS in general. The Para site (235 varves) corresponds to 3303 to 3069 cal BP (Table 4 and Fig. 11).

The varve section of Västeraspby, Stockhed, Nordsjödike are not connected to the existing timescale. These series contain little variation and the Stockhed series contains hiati. Nordsjödike is located in a separate tributary, Stockhed is most likely an equivalent of Björkå bruk, Västeaspby is likely an equivalent of Korvsta. However, as long as these floating chronologies are not constrained by either delta surfaces or elevation in the bluffs there is no value in attempting to connect them to the existing time scale.

Table 4. Five new varve series and their connection to the STS

Site	Position	Length years	Varve chronology BP
Sollefteå_98 #	63,10,00 N; 17,19,00 E	158	4955–4799
Para #	63,11,00 N; 17,31,05 E	234	3303–3069
Vesteaspby	63,10,00 N; 17,29.05 E	99	N/A
Stockhed	63,10,00 N; 17,36,00 E	c. 154	N/A
Nordsjödike *	63,12,00 N; 17,01,00 E	104	N/A
Sollefteå_97 §	63,10,00 N; 17,19,00 E	489	4415–4903

Table 4. New varve series. * located in the Faxälven tributary. # Series connected to Cato - Lidén's varve chronology, § varve series published by Wohlfarth *et al.* (1997). Positions of new varve series are showed in Fig. 9.
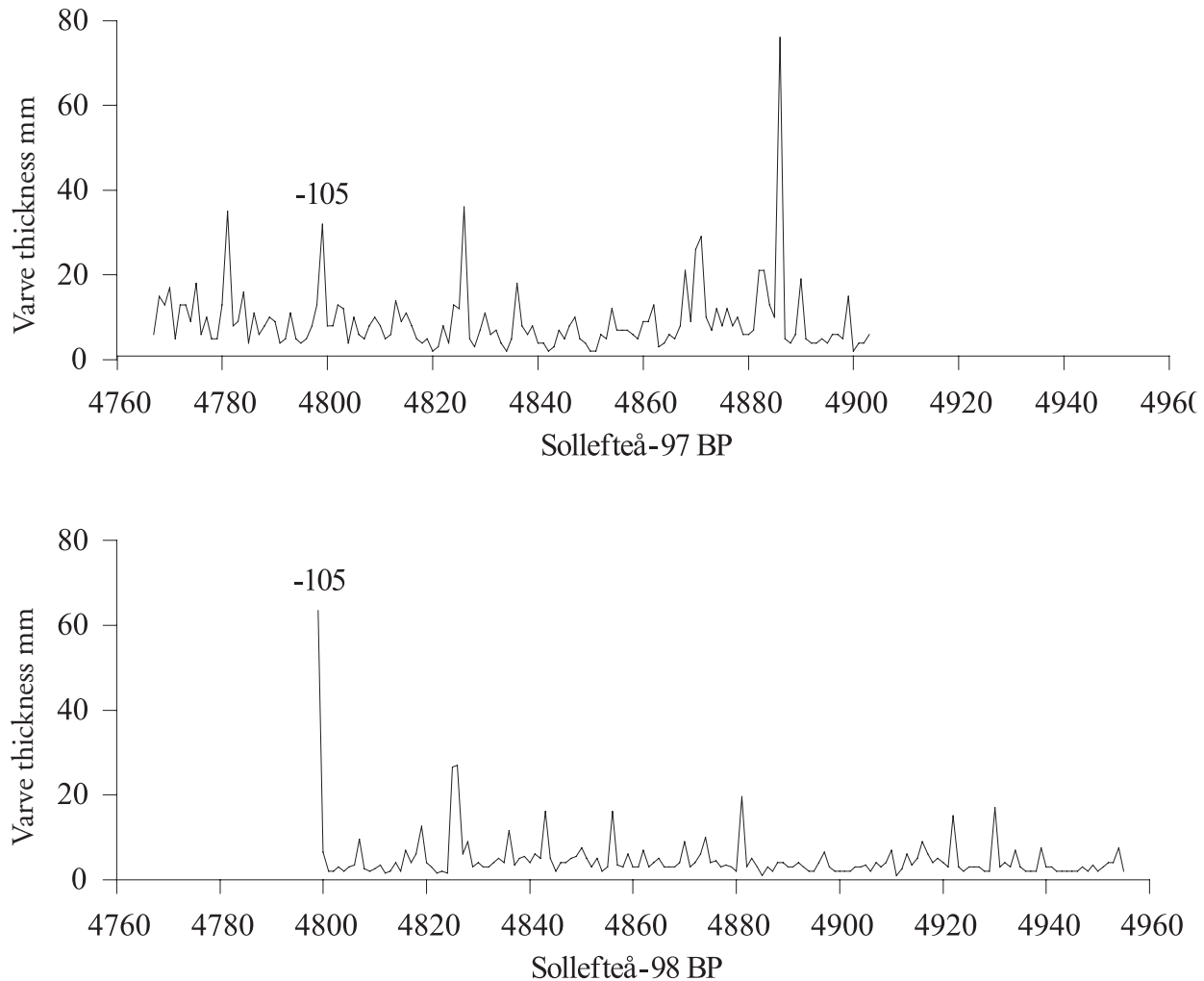
Fig. 10. *The Solleteå-98 connection to Sollefteå-97. Top panel the Sollefteå-97 series, lower panel the Sollefteå-98 series. The Sollefteå-97 continues further forward in time than showed. The −105 varve is marked which according to description (see text) corresponds to the youngest varve of Sollefteå-98.*

7.2 Cross-correlation of R. Lidén's series

It has been argued that a considerable amount of time (500–875 years) is unaccounted for in the existing STS, due to so-called "missing" varves (e.g. Wohlfarth and Possnert, 2000). Based on radiocarbon dating a ca 500 year error is suggested in the 2000–5000 BP period. A "missing" varve problem could be caused by either varves that remain unmeasured or to false connections within the existing varve chronology. The sites measured by R. Lidén were in the near vicinity of each other (Cato, 1998) and, therefore, it is most unlikely that any varves escaped measurement. Hence, the problem is probably related to false connections. R. Lidén, however, based part of his argumentation on the elevation of delta surfaces as the delta moved eastwards, which does not initially allow for an error in the connections comparable to the potential gap. With a con-servative average varve thickness of one centimetre, c. 500 years would correspond to a single sediment thickness of c. 5 metres, which is unlikely to have been overlooked.

Several studies have pointed towards discrepancies between the varve age of the multiple section STS and ages obtained by other means, such as radiocarbon dating (e.g. Andrén *et al.*, 1999; Björck *et al.*, 1987; Björck *et al.*, 1995; Holmquist and Wohlfarth, 1998; Wohlfarth, 1996; Wohlfarth *et al.*, 1997; Wohlfarth *et al.*, 1993; Wohlfarth and Possnert, 2000). A comprehensive analysis of radiocarbon dates obtained from Swedish clastic varves is presented in Wohlfarth and Possnert, (2000). In addition, direct correlation to GRIP ice core to the glacial part of STS reveals that varves in the order of 700–900 years are missing in the varve chronology at the Younger Dryas–Preboreal transition (Björck *et al.* 1996 and Andrén *et al.*, 1999). On the other
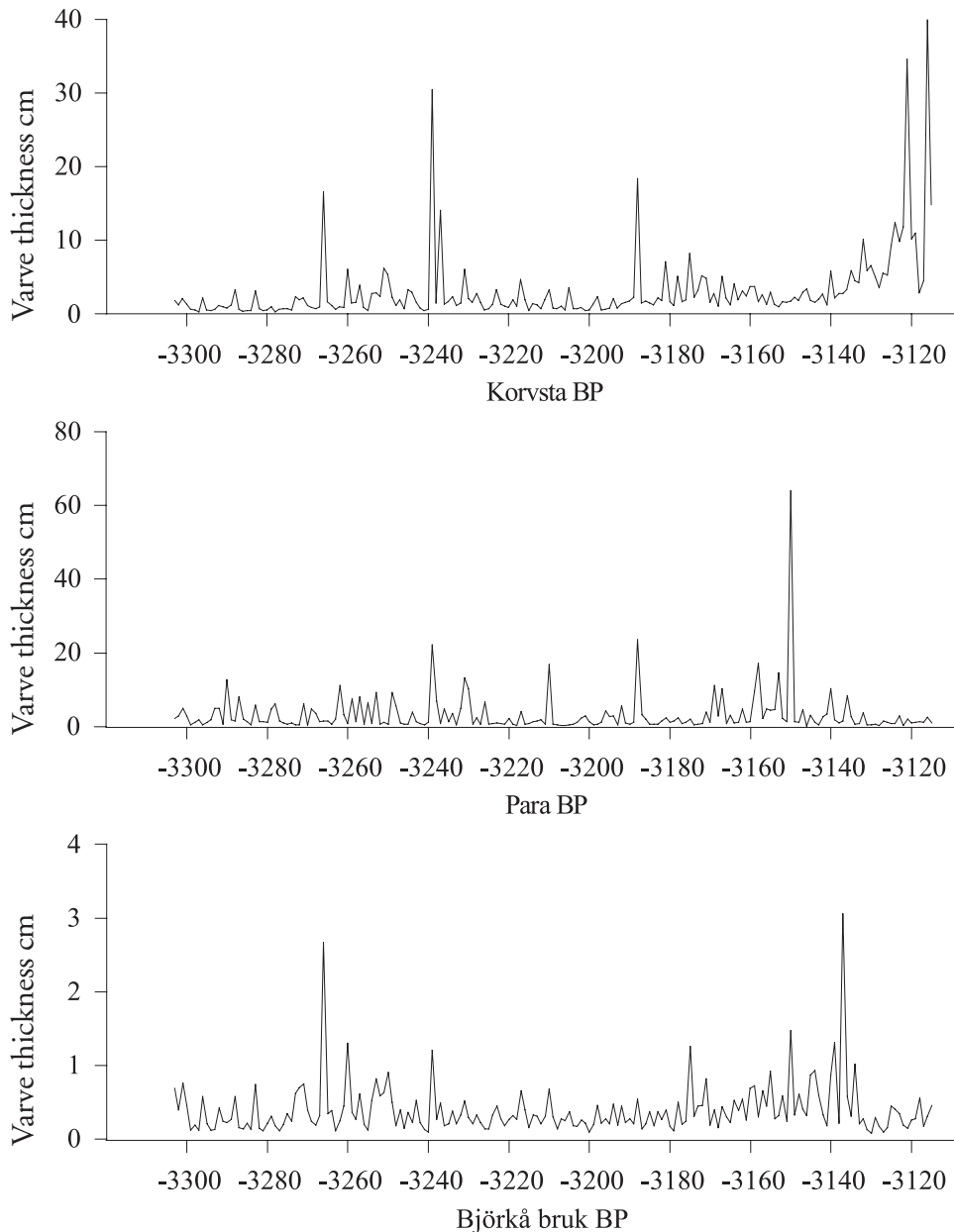
Fig. 11. The Para series connection to Korvsta and Björkå bruk.

hand, absolute faith cannot necessarily be placed in the GRIP ice core chronology. The accepted STS is based on the visual and potential subjective connection of varve diagrams. In the following all connections are tested by an independent and objective statistical means, i.e. cross-correlation analysis.

It must be stressed that Cato (1987 and 1998) slightly modified the raw data by adding and subtracting years. This practice generates a problem for the cross-correlation analysis if any of the corrections were wrong. On the other hand if the corrections consistently eliminate true double varves and varves missed the value of the cross-correlation analysis will be enhanced.

A review of all published varve diagrams from the River Ångermanälven has been carried out (Table 5 and App. V). Some varve sections hold substantial hiati, which are poorly covered by adjacent varve series. Two options can deal with the absence of data. Either the gaps are filled with blanks and the analysis performed on the entire time span of overlap, or the subperiods in which the two series both are represented with data are extracted. Both options were applied.

The varve chronology between 1850 A.D. and 1978 A.D. has previously been validated (Wohlfarth *et al.*, 1998). Before 1850 A.D. and throughout the chronology collected by Cato, (1987) all connections are valid. The cross-correlation was done

Table 5. Cross-correlated diagrams

Varve series cross-correlated	Connection valid?	Comment
Nämforsen vs. Mo	pass	
Mo vs. Omnäs	pass	
Omnäs vs. Myre	pass	
Myre vs. Vignäs	pass	
Myre vs. Forsmo	failed	#
Vignäs vs. Forsmo	pass	
Vignäs vs. Sand	pass	
Forsmo vs. Sand	pass	
Sand vs. Ön	pass	
Ön vs. Rödskägget	pass	
Rödskägget vs. Risöviken/S	failed	*§
Risöviken/S vs. Sotdalen	pass	*
Risöviken/S vs. Nyland	failed	*§
Risöviken/S vs. Risöviken/M	pass	*
Risöviken/S vs. Färjestället	pass	*
Risöviken/M vs .Nyland	pass	*
Risöviken/M vs. Färjestället	pass	*
Nyland vs. Färjestället	pass	
Färjestället vs. Sågån	pass	
Sågån vs. Korvsta	pass	
Sågån vs. Björkå	failed	#
Korvsta vs. Björkå	pass	
Björkå vs. Undrom	pass	
Undrom vs. Prästmon	pass	† older part
Undrom vs. Prästmon	failed	† younger part

Table 5. Cross-correlation encompassing total length of series i.e. internal hiatus filled with Not a Number values. Additional analysis on sub-segments that contains data were preformed in some cases, see § and †.

*Risöviken/S: Risöviken Sollefteå, and Risöviken/M: Risöviken Multrå.

These connections are considers invalid by cross-correlation analysis, but other series covering the same period are valid connected.

§ These connections are not valid cross-correlating the total overlap. Six unique cross-correlations were subsequently performed on the Risöviken/S vs. Rödskägget overlaps and one cross-correlation on the Risöviken vs. Nyland that contains data in both series. These seven new cross-correlations support the original chronology by Cato (1998).

† The Prästmon section is divided by an internal hiatus of 36 years, the younger respectively older part has been cross-correlated to Undrom.

prior to the calculation of the geometric mean utilized in this Thesis (Holmquist unpublished). The connection between Cato's Prästmon section (Cato, 1987) and R. Lidén's Prästmon section (Cato, 1998) is validated. Problems emerge when the chronology

constructed by R. Lidén on raised deltas are analysed. Many of the varve sections have hiatus of varying lengths, which hamper the cross correlation exercise.

The lack of a significant SNR is identified in the connection of the full overlap of Risöviken/S–Nyland, Rödskägget–Risøviken/S and Undrom–Prästmon (Table 5). However, these series have many hiatus that were filled with blanks for the statistical test. When the actual overlaps that contain data were tested in the many sub-segments significant SNR are detected in all but one (App. V). Thus, the Risöviken/S–Nyland and Rödskägget–Risöviken/S connections are considered robust. In the Undrom–Prästmon connection the mismatch is confined to the younger part of the connection overlap (a hiatus of 36 years due to indistinct varves divides the Prästmon series into two sections). It is possible that the most recent part of Prästmon is falsely connected to Undrom. However, due to the vertical measurement technique (De Geer, 1940) it seems unlikely that 500 years (5 m) could be omitted in a 36 year gap. The cross-correlation does not reveal any alternative connection. The current connection between Undrom and Prästmon, drawn as skeleton plots (Cato 1998), appears convincing.

Apparent contradictive arguments emerge because the two methods utilize different approaches. The skeleton plots (used in classical varve diagram connection) focus on the pattern of markers (thick varves), whereas the cross-correlation takes all data pairs into account. The many annual pairs of thin varves do not support a significant linear regression, but rather a sphere of varve pairs. The Prästmon series of R. Lidén has been validated by the study of additional foil cores (Cato, 1987). The failure of any significant SNR in the most recent overlap between Undrom and Prästmon is most likely due to the abnormal proximal varves in the most recent part of the Undrom series.

The "missing" varve of the post glacial part of STS remains a mystery. The post-glacial period seems to be robust. An error in the order of c. 500 years cannot go undetected with the close distance between varve sites and the constraint of delta surfaces. In addition the vertical constraint (varves are measured vertically in cores and bluffs), negate the suggestion that a centennial error can lurk in the many hiatuses some of the records contain.

Some doubt could perhaps be raised concerning the validity of the postulated "missing" varves. Radiocarbon dates can be unreliable (e.g. Oldfield *et al.*, 1997; Wohlfarth *et al.*, 1998), despite the omnipresent use of calibrated "calendar BP" dates the reality behind any C–14 date is a statistical distribution, either of beta counts of a count of the

number of particles (AMS). Regardless of the calibration by tree-rings series, the date remains a pure probability assessment, never an absolute age.

Calibrated radiocarbon dates (Wohlfarth *et al.*, 1997) may not be sufficient to claim a 300–875 (500) year error in the STS between 2000–5000 BP. The argument was based on one terrestrial macrofossil obtained from c. 3–5 kg of sediment. This sample (Ua–11230) consisted of a single *Betula* seed and catkin scales, with a mass of 1.7 mg. It is this one date (5730–5040 BP calibrated) that led the authors to claim a centennial-scale fault in the 5000–2000 BP period of the STS (Wohlfarth *et al.*, 1997). A recent tephrochronological study of varve-lake sediments in Värmland, Central Sweden, by Zillén *et al.* (2002) indicates the problems associated with comparing AMS macrofossil dates with a varve chronology with the AMS-^{14}C technique. (i) The fact that delta structures are composed of re-deposited material (Cato, 1998), (ii) the curious absence of macrofossils, which should alert any careful use of radiocarbon dates, is not discussed. The authors analysed 24–40 kg of sediment and retrieve 2.7 mg in total of terrestrial organic material of which 1.7 mg are analysed. Approximately, one half of the radiocarbon data extracted from varves clays in Sweden has been disregarded as unreliable (Wohlfarth and Possnert, 2000, Wohlfarth *et al.*, 1993). However, it must be acknowledged that remaining radiocarbon data persistently indicate an age difference between the radiometric time scale and the varve chronology i.e. radiocarbon dates being older than the stratigraphical varve date.

The missing varve assessment advocated in Andrén *et al.*, 1999 is based on a comparison between the radiocarbon age of the palynologically determined Younger Dryas–Preboreal boundary in varved clays and the age of the Pleistocene/Holocene boundary in the annually layered GRIP ice-core; the latter defined by its oxygen isotope composition. The argument that GRIP oxygen isotope composition and the pollen content of varves in the Baltic proper exhibit strictly synchronous development can be questioned. It may be argued that the low number of low pollen samples measured (11) and the rather uniform vegetation with many species only represented by less than 1% of the pollen sum is not sufficient to allow a biostratigraphic definition of Younger Dryas–Preboreal boundary. Moreover the Younger Dryas–Preboreal boundary in the GRIP ice core is defined arbitrarily at the point where the δ^{18}O value passes above –40 per mille.

In order to solve the problem of potential missing varves, independent means of synchronising the STS and other geological archives are necessary. One possibility is tephrochronology, which has been widely used in the North Atlantic and northern Europe (Wastegård unpublished) and has be en applied to varved lake sediment in Sweden (Zillen *et al.*, 2002). The Vedde ash has already been found in sections of the STS (Wohlfarth *et al.*, 1993). The River Ångermanälven catchment is located downwind from Iceland and collects material from a vast area and deposits an annual layer in the estuary. Given the large catchment area there is a large probability that volcanic glass shards could potentially accumulate in the delta structure and provide an independent assessment of age. Of course, the redeposition of old delta material structures would likely spread glass shards to the entire chronology, but the outfall year should be marked as peak signal of shards on the background of redeposited shards (Wastegård unpublished).

7.3   Missing varve in the post glacial?

It was anticipated that the five new varve diagrams presented here would help solve the "missing" varve problem (Wohlfarth *et al.*, 1997). However, of the five diagrams only two are considered to possess variability that facilitates connection to the existing chronology. A new series form Sollefteå is connected to a previously published Sollefteå series (Wohlfarth *et al.*, 1997) and adds c. 50 years to the summed series. A series from Para is connected to two neighbouring series, Korvsta and Björkå bruk. None of these series contains data that facilitate an extension of the existing chronology (Cato, 1998). A full evaluation of all the connections by statistical means confirmed the majority of the connections. Scrutiny of the few weak connections revealed that only one connection was invalid, i.e. the most recent part of Undrom–Prästmon connection. However, the older part is well correlated and it is inconceivable that an extra c. 500 years could be added to fill the Prästmon hiatus. No other valid connection between these two series was indicated by cross-correlation. Thus, it is concluded that there is no concrete evidence for a centennial error in the post glacial section of the STS. The persistent deviation between ^{14}C dates and varve dates constitutes a problem, but it is most likely that the problem concerns the reliability of ^{14}C dates obtained from a geological material poor in organic remains, rather than the validity of the varve chronology.

8.0 Frequency analysis of R. Lidén's series

Paper III demonstrated that some persuasive frequencies are present in the series of geometric mean varve thickness for the past 2000 years. The presence of cycles in varved deposits was further investigated in the R. Lidén series from River Ångermanälven (Cato, 1998). The frequency analysis was carried out on individual sections as no mean based on multiple segments was calculated. As the frequency analysis cannot handle internal absence of data the varve data series containing internal hiatus were analysed in sub-segments. Sub-segments shorter than 100 years were not analysed, nor were the proximal varves.

The presence of sub-decadal, decadal and centennial frequencies in the geometric mean series for the past 2000 years indicates that the same frequencies are present in the individual varve diagrams. Anticipating that the fluvial system does not change in its response to forcing with quasi-stationary frequencies, i.e. NAO, Schwabe cycles and Suess, these frequencies should be persistent in the entire post glacial period.

A wide range of frequencies is present in the 19 varved sites measured by R. Lidén (Table 6 and App. V). Sub-decadal frequencies dominate in all sections and these are tentatively correlated to inter-decadal precipitation variations mainly forced by changes in the atmosphere (NAO and Lamb). The NAO accounts for a significant part of the winter precipitation variation and the temperature variation (Chen, 2000; Chen and Hellström, 1999).

Decadal frequencies detected in the 10–15 year band are cautiously connected to solar variation of the Schwabe cycle. The Schwabe cycle is responsible for the well-known sunspot cycle (11 years) and the physical parameters that alter are connected to the Sun's magnetic field, particle flux, corona temperature, irradiance spectrum, etc. The climatic forcing potential of minute variations (c. 1 per mille) in the solar energy flux during a sunspot cycle has been widely discussed (Björck *et al.*, 2001; Haigh, 1996; Rind, 2002; Svensmark and Friis-Christensen, 1997). A number of varve sections contain frequencies in the 20–25 and 66.67 year band, which can speculatively be connected to the Hale cycle and the Gleissberg cycle, respectively. The Gleissberg cycle is normally set to around 80 years, but given the fixed frequency style of the periodogram there is a slight possibility for a detection of a longer 0.015 cycle pr year (66.67 year frequency). The next frequency to be checked in the periodogram is the 0.010 cycle pr year (100 year frequency). In most of the varve sections a persistent centennial frequency is detected.

Centennial variability is speculatively connected to the Suess cycle.

In general, the frequencies detected in the individual series of R. Lidén are comparable to the result of Paper III. A fast frequency domain dominated by NAO, a decadal band forced by solar variation and a slow frequency tentatively connected to the Suess cycle.

9.0 Discussion

9.1 Climate – environment overview

The climatic responses to future greenhouse gas emissions has been evaluated in innumerable numerical models on local, regional and global scales on a multitude of time scales. Although temperature variability and ice-sheet changes receive the lions share of attention, the most profound impact of climate change for humans is the rearrangement of the hydrological cycle.

The hydrological changes take many forms; increased temperature increases the strength of the hydrological cycle, i.e. more water in the atmosphere, precipitation, and evapotranspiration and discharge. Thus creating a generally wetter environment. However, it is a case of equilibrium, potential evapotranspiration can be in the order of potential precipitation and create semi-arid areas (Watson and Coregroup 2001).

Despite a generally wetter climate initially extreme events will decrease in central Sweden. This is because extreme discharge events are related to snowmelt water pulses, which will be reduced in a warmer climate. Thus, the predicted local influence of future climate change on River Ångermanälven is a decreasing trend in the SMF but a net annual discharge increase. As such it will influence the management of hydro electrical installations and the scaling of future constructions.

The relationship between climate change and discharge has been verified in this study and others (Cato, 1987) by the close agreement between the SMF variation inferred from varve thickness and the late Holocene climate succession. For a future scenario SMF events will likely decrease to the level of the MWP. Strengthening the hydrological cycle beyond that of the MWP will likely increase the maximal discharge event by shifting from spring meltwater induced to autumn storm-induced discharge events. Perhaps a climatic mode which is already active, inasmuch as a number of destructive high water levels in River Ångermanälven during the 1990's,

Table 6. Frequencies in R. Lidén's varve series

	Nämforsen	Mo	Omnäs	Myre	Vignäs	Forsmo	Sand	Ön	Rödskägget	Sotdalen
Sub decadal	5.80 2.25	3.03	2.50 3.57 6.25 9.52	2.35 2.47 4.17 5.26 6.25 6.90 8.7–10.00	2.35 2.44 2.99–3.03 4.17	2.44 3.03 3.3	2.56 2.85 3.85 7.69	2.94 3.64 6.06 6.90 7.69 8.70	2.20 3.13 8.33	2.38 2.86 3.08
Decadal	11.76 66.67	22.22	11.11	11.11 83.33	10.53 33.33	10.53	13.33			22.22 28.57
Centennial	200	200	200	200	200	100	200	200	100	200

	Risöviken/S	Risöviken/M	Nyland	Färjestället	Sågan	Korvsta	Björkå bruk	Undrom	Prästmon
Sub decadal	2.17 2.22 3.17 6.66–6.90	2.90 5.26 9.52	2.22 2.47 2.67 2.86 3.08 4.17 4.35 8.70 9.52	3.08 3.77 4.88 5.26	2.35 2.53 5.71 6.25 7.69 9.52	2.04 2.20 2.56 2.67 2.94 7.14	3.92 4.35 4.76 5.13	2.30 2.44 2.56 2.94 4.35 6.06 6.90	2.20 2.25 2.56 2.94 3.03 4.55 5.41 6.45
Decadal	10.53 13.33–14.29 33.33	15.38 25.00	15.38 29.41	66.67	66.67	13.33 15.38	66.67	18.18 66.67–200	13.33 22.22 50.00
Centennial	200	100	100			100			200

Table 6. Significant frequencies detected in the post glacial varve series measured by R. Lidén (Cato, 1998). Frequencies were detected by periodogram see App. V

has occurred in the autumn (http://www.smhi.se/sgn0102/n0205/oversvam/1993_1.htm). However, conclusions on the response to rainfall events must evaluated in the light of the extensive regulation, i.e. the discharge peak produced may be an effect of river management rather than extreme rainfall. Hydrological models can easily resolve this question.

The varve record is transformed into the best possible discharge (SMF) series through a power equation. The power equation ensures that extreme varve thickness is reasonable within the predicted natural variation. A considerable part (c. 40%) of the SMF variation is linked to the AAWP, thus a climate control is evident. AAWP is to some extent controlled by NAO, but the atmospheric signal is not detectable in the reconstructed SMF variation. The long centennial trend of the reconstructed SMF series is closely associated to the Late Holocene climate succession, RWP, DACP, MWP, LIA and CWP. A number of frequencies were detected in the varve series, a fast frequency band associated with atmospheric/ocean variability, an intermediate frequency band forced by the solar Schwabe cycle and a centennial frequency band tentatively connected to the Suess cycle.

9.2 The temperature signal

The additional analyse present herein have not disclosed any new major forcing parameters or co-variation in relation to the varve thickness. Discharge is derived from melting of snow pack, but no pervasive temperature signal is detected. Six temperature series from within and outside the catchment have been scrutinized on monthly and seasonal timescales (App. V). The absence of any significant temperature signal in the varve series is likely due to the distinct character of the temperature signal. The melt water that enters the fluvial system has to pass through a number of sub-basins before being released to the fluvial system. Initially the first melt water is withheld in the snow pack, which can accommodate ~10% water equivalent. Thus, 10% of the snow pack's melt water (and temperature signal) is withheld and not directly detectable in the SMF. To further complicate the process freezing may occur during night, resetting thawing. When the temperature rise finally produces melt water that escapes the snow pack, the water enters the soil (if it is not frozen). The soil can withhold water to field capacity; when field capacity is exceeded melt water forms overland flow. At the same time, melt water reach the groundwater reservoir, which feeds the fluvial system. The melt water generation process is amalgamated for the many sub basins and finally make up the SMF pulse at Sollefteå. In order to distinguish a

temperature signal in the varve series it is paramount to obtain a temperature series that accommodates the year-to-year variability of the above described process.

9.3 Tree-rings

Tree-rings series could potentially share some variability with varve series due to the seasonal resolution and a summer temperature and an autumn precipitation signal. One significant correlation between a local tree-ring series and SMF was found. However, this tree-rings series proximity to the coast is problematic, since major melt water volumes are seldom released from the coastal region into the estuary. Generally it must be questioned if tree-rings are linked, through a common driver, to varve thickness.

The Torneträsk tree-ring series shares some variability with the SMF record especially in the long-term trend. However, the correlation is positive, thus warmer climate *sensus* Torneträsk tree-rings are tied to increasing varve thickness, in opposition to the forcing process as perceived in previous publications (Paper III) and by numerical models (Gleick, 1989). Likely the sub-artic climate as resolved in the Torneträsk tree-rings series are not directly comparable to climate parameter(s) involved in varve formation in central Sweden.

9.4 Atmospheric circulation

The atmospheric circulation is a major driver of the winter precipitation variation in Ångermanland and thus potentially of SMF. Three atmospheric indexes have been compared to SMF, (i) the NAO, (ii) geostrophic wind and (iii) vorticity. The geostrophic wind shares a considerable variation with monthly discharge, however the co-variation is a result of strong seasonality in both series and thus does not in itself indicate a causal link. Any proxy with inter-annual seasonal variation would share variability with an inter-annual discharge record from central Sweden.

The influence of an "annual" geostrophic wind mean is an important topic in the context of SMF. To what extent is the year-to-year numerical variation in the geostrophic wind reflected in the annual SMF? A mean geostrophic wind calculated based on the hydrological year turn out to be insignificantly correlated. Two extreme annual series can be extracted from the monthly geostrophic wind series, the minima and the maxima. The series of minima represent the summer geostrophic wind and is uncorrelated to SMF. The maxima series are mainly derived form winter geostrophic wind and it is significantly correlated to

SMF. However, in some cases maximum winter geostrophic wind is extracted from late in the calendar year and, therefore lags one year in comparison to the SMF. Thus, the maxima series of geostrophic wind is not directly comparable to SMF, although the calculated correlation is pervasive. A strong zero time lag forcing of geostrophic wind on monthly precipitation has been demonstrated.

NAO is a major driver of winter precipitation variation in Ångermanland although the signal of the NAO is not preserved through the melt generation and the resulting SMF. A NAO reconstruction (Cook *et al.*, 1997) also proved to be insignificantly correlated to SMF. It must be concluded that atmospheric circulation variability may effect precipitation but the signal is overridden by noise generated during melt and confluence of the flow derived from the many sub-basins.

9.5   Global temperature reconstructions

The comparison between varve thickness and various global temperatures reconstructions should be interpreted with caution. Both the Northern and Southern component of the Jones (1998) and Briffa (1998) global temperature are significantly correlated with the SMF (51 year running mean). Note that the calculation of correlation coefficients on averaged series is a violation of the prerequisite of independent data. Any point in the 51 year windows averages are dependent upon 25 neighbouring data points in each direction. Thus the r-value itself is meaningless but it naturally indicates some sort of co-variation in the proxies.

The fact the Jones (1998) Southern hemisphere temperature is better correlated to reconstructed SMF than the Northern hemisphere clearly indicates that the heedless use of correlation coefficients are pointless. The negative correlation coefficient is in accordance with the perceived structure of general climate influence of SMF. The positive correlation between Briffa (1998) global temperature and SMF reconstructed is in opposition to the perceived connection between long-term temperature changes and AAWP/SMF.

9.6   Baltic sea-ice and volcanoes

Annual maximum Baltic sea-ice extent is to some degree controlled by NAO, as is the winter precipitation that is the precursor to SMF. But SMF and Baltic sea-ice extent do not share any variability. Varve years concurrent with major volcanic eruptions appear to be persistently thinner but a statistical test could not support this preliminary observation.

Since volcanoes have a cooling effect on global temperatures, the opposite relation was expected i.e. a volcanic forcing of thick varves.

9.7   Missing varves and frequencies in the older part of the STS

It has for some time been argued that a considerable amount of time is missing in the STS, both in the post glacial period and in the older fini- and goti glacial period. All connections between varve sections in the post glacial have been tested by statistical cross-correlation, a few was found to be statistical invalid, these were tested in detail. Only one connection, Prästmon–Undrom the most recent part, could not be supported by statistical analysis. However the connection between Prästmon and Undrom is valid in the older parts, thus it seems unlikely that a centennial error is hidden in the Prästmon series. Two new series have been connected to the existing chronology (i) extension of the series previously obtained from Sollefteå (Wohlfarth *et al.*, 1997) by c. 50 years, (ii) a new series from Para was fitted to Korvsta and Björkå bruk series (Cato, 1998).

The most recent 2000 years of the STS holds frequencies on inter decadal, decadal and centennial band (Paper III). Frequency analysis on the individual varve sections measured by R. Lidén (Cato, 1998) showed that the frequencies of the same bands are present in the older part. These are tentative connected to ocean-atmosphere (NAO) variability for the fast frequencies (inter decadal). Solar forcing, Schwabe cycle, for the frequencies around 10 years. Speculative the centennial frequencies are related to the Suess cycle. The detection of 66.67 year cycle could perhaps be linked to the Gleissberg cycle.

10.0   Conclusions

The climatic significance of the Late Holocene part of the STS has been investigated. The varves mathematical relationship to discharge has been unravelled and a long robust maximum discharge series (2000 year) has been reconstructed. The maximum discharge events of Ångermanälven are exclusive to the snowmelt flood (SMF), thus the reconstructed series is tied to the snowmelt process (Paper I).

Winter precipitation from 11 stations within and in the near vicinity of the watershed was accumulated and the variability of each tested for co-variation with the reconstructed SMF. Two stations did not share any variation and were excluded; the remaining stations were averaged into a mean, average accumulated winter precipitation (AAWP) (Paper II).

AAWP accounts for ~40% of the variation in the SMF. This is not enough to justify an annual calculation of AAWP based on varve thickness, but sufficient to associate the long trend of the SMF series with variation in the long trend winter precipitation. Ascertained on the precipitation signal in the SMF series the classical (Europe) Late Holocene climate successions evident, Roman Warm Period, Dark Ages Cold Period, Medieval Warm Period, Little Ice Age, and Contemporary Warming.

Comparing the reconstructed SMF to the GISP2 oxygen series reveals a curious phenomenon. Due to the NAO seesaw an anti-phase relationship is expected between the two proxies, which is confirmed from the present until 1700 A.D. The relationship predating 1700 A.D. is in-phase, indicate that the NAO was absent/inactive (Paper II).

Frequencies in the 2–5, decadal and centennial band were detected in the 2000 year long SMF series. The fast periodicity is tentatively linked to variability of atmosphere/ocean (NAO). The intermediate (10 year) is in antiphase with the observed sunspot number and suggests the presence of a solar forced Schwabe cycle in the varve thickness. The centennial periodicity is tentatively linked to the Suess cycle. These sub millennial frequencies are superimposed on a longer millennial waveform, which is probably associated with the Bond cycle (Paper III).

Despite an all-inclusive understanding of the snowmelt flood processes and the influence of temperature variations, it has not been possible to demonstrate any temperature co-variation. This is because the temperature series that forces the year-to-year variation in SMF is elusive and unlikely grasped by the monthly or seasonal temperature series.

Contradictive and non-conclusive results were obtained from comparison with the SMF (observed and reconstructed) and varve thickness and the following proxies: Temperature series from Stockholm, Uppsala, Junsele, Härnösand, Stensele, Forse and Gäddede, five local tree-ring series and Torneträsk, atmospheric indices, NAO, geostrophic wind, vorticity and a NAO reconstruction, annual maximum Baltic sea-ice extent, global temperature reconstructions of Jones and Briffa, and volcano eruptions above VEI 5.

11.0 Svensk sammanfattning

Denna avhandling handlar om hur man kan utläsa klimatiska signaler från klastiska årsvarviga sediment i Ångermanälven i södra Norrland. Avhandlingen bidrar med kunskap till den pågående diskussionen om klimatets- och den hydrologiska cykelns föränd-ringar, framförallt sett ur ett retrospektiv men den behandlar också frågor om framtiden och en eventuellt ökande växthuseffekt.

Varviga sediment förekommer längs den svenska östkusten och i Sveriges norra- och centrala dalgångar. Tillsammans utgör dessa sediment en lång tidsskala, den så kallade Svenska Tidsskalan, som sträcker sig från nutid genom hela vår nuvarande värmetid (Holocen) och in i slutet av den senaste istiden (Senglacial tid). Varven har avsatts i två olika miljöer (1) dels framför den retirerande Fennoskandiska inlandsisen i en issjömiljö och (2) dels i dalgångarna efter att inlandsisen hade dragit sig tillbaka efter isavsmältningen i en lakustrin miljö. Denna avhandling fokuserar främst på varven i Ångermanlandsälvens dräneringsområde som har bildats under de senaste ca 2000 åren men den behandlar även de varv avsatta de senaste 8000 åren. Tidsintervallet valdes på grund av att preliminära analyser visat att tidsskalan är tillförlitlig och för att det i sedimenten i mynningen av Ångermanälven finns varv som bildats under denna period.

Endast i ett fåtal tidigare undersökningar har förhållandet mellan varvtjocklek och vattenflöde studerats. I denna studie har ett säkert samband mellan varvtjocklek och observerad maximal dagligt årsflöde (Qmax) för åren 1909–1971 upprättats. Förhållandet mellan de två parametrarna har uttryckts med en potensekvation, vilket underlättat beräkningen av Qmax för de senaste 2000 åren. Tidsserier av Qmax har analyserats en efter en. Jag fann bl. a. en tillfredsställande fördelning av de extrema värdena i jämförelse med observerade dataserier. Qmax visade sig också sammanfalla med vårfloden, vilket betyder att förändringarna i varvtjockleken beror på variationer i snösmältningen. Observerad och rekonstruerad Qmax har korrelerats till observerat snömedeldjup, vilket visar att Qmax är ett resultat av mängden smält nederbörd i form av snö. Detta betyder i sin tur att det finns signaler i varven som leder till variationer i atmosfären.

I årsnederbördsdata upptäcktes en vintersignal i den s.k. ”North Atlantic Oscillation” (NAO), vilken inte kunde urskiljas i varken Qmax eller varvtjockleken. Jag fann att en hundraårig periodicitet i varvtjockleken sammanfaller med den klassisk Senholocena klimatutveckling dvs. med en varm period under romartiden, en kall period mellan ca 500–1000 e. Kr., åter en varm period under Medeltiden följt av ett kallt klimat under den Lilla istiden och slutligen uppvärmningen i vår egen tid.

Om det finns en atmosfärisk faktor som påverkar bildningen av varv ska det vara möjligt att sammankoppla varvtjockleken till andra arkiv som påverkas av atmosfären t. ex. variationer i O^{18}/O^{16} halten i den

Grönländska inlandsisen. Enligt instrumentobservationer och de mekanismer som påverkar NAO, borde det finnas ett omvänt förhållande mellan de två temperaturkänsliga arkiven. Ett sådant förhållande upptäcktes i varvserien under vissa tidsperioder men inte under andra. Detta av- och på förhållande har tolkats som start- och slutsignaler för NAO.

Baserat på frekvensanalyser har jag visat att tidsserierna innehåller icke-stationära solvindscyklar men också andra frekvenser. Förutom solvindens cyclicitet, upptäcktes periodiciteter som sträcker sig från tiotals till tusentals år, vilka kan kopplas till variationer i t. ex. NAO och Suesscykeln. En 1000 års lång vågform har spekulativt kopplats ihop med Bondcykeln, som hittats i marina sediment.

Förutom dessa analyser utfördes ytterligare ett antal analyser för att kunna utreda förhållandet mellan varvtjocklek, Qmax och andra arkiv som kan innehålla indirekt information om klimatets variationer. Dessa arkiv utgjordes av trädringsserier, temperaturserier, atmosfäriska data, isutbredningen på Östersjön, kol-14 serier och data från vulkanutbrott. Slutsatserna från dessa korrelationsanalyser var i huvudsak negativa, dvs. jag fann inget samband mellan varvtjocklek och de andra arkiven.

Jag har även gjort försök med att korrelera olika varvserier omfattande de senaste ca 8000 åren eftersom tidigare upptäckter visat att kronologin i den Svenska Tidsskalan kombinerat med kol-14 dateringar av organiskt material som påträffats i lervarven och tidskalan i en borrkärna från den Grönländska inlandsisen (GRIP borrkärnana) inte överensstämmer och att det saknas minst 500 varv i den Svenska Tidsskalan. Mina resultat pekar på att de saknade varven troligtvis inte går att finna i Ångermanälvens avlagringar.

Denna avhandling har ökat kunskapen om varv i Ångermanälven på ett flertal olika sätt bl. a. genom att:

- sambandet mellan Qmax och vårfloden har utretts
- varvdata har omvandlats till vattenflödesserier
- en hundraårig periodicitet har tolkats inom ramen för klassisk Senholocen klimatutveckling
- frekvenser sammankopplade till NAO, solvindscykeln och Suesscykeln har upptäckts
- tidsskalan har granskats med hjälp av korrelationer och förklarats tillförlitlig
- flera olika klimatiska arkiv har testats gentemot varvtjocklek, men dessa studier gav inget nytt ljus åt förståelsen om hur varven i Ångermanlandsälvens dräneringsområde varierar

References

Andrén, T., Björck, J. and Johnsen, S., 1999. Correlation of Swedish glacial varves with the Greenland (GRIP) oxygene isotope record. *Journal of Quaternary Science,* 14: 361–371.

Arnborg, L., 1958. *Nedre Ångermanälven.* Publications from the Geographical Institute, University of Uppsala, Uppsala.

Arnborg, L., 1959. *Nedre Ångermanälven. 2,* Publications from the Geographical Institute, University of Uppsala, Uppsala.

Bengtsson, L. and Iritz, L., 1990. Climate change and floods in northern basins. *International conference on river flood hydraulics,* pp. 307–316.

Bergsten, F., 1954. The land uplift in Sweden from the evidence of the old water marks. *Geographical Annals,* 36: 81–111.

Bergström, S., 1992. *The HBV model – its structure and applications.* RH No. 4, SMHI, Norrköping.

Bianchi, G.G. and McCave, N., 1999. Holocene periodicity in North Atlantic climate and deep-ocean flow south of Iceland. *Nature,* 397: 515–517.

Björck, S., Sandgren, P. and Holmquist, B., 1987. A magnetostratigraphic comparison between ^{14}C years and varve years during the Late Weichselian, indicating significant differences between the time-scales. *Journal of Quaternary Science,* 2: 133–140.

Björck, S., 1995. A review of the history of the Baltic Sea 13,0 to 8,0 ka BP. *Quaternary International,* 27: 19–40.

Björck, S., Kromer, B., Johnsen, S., Bennike, O., Hammerlund, D., Lemdahl, G., Possnert, G., Rasmussen, T.L., Wohlfarth. B., Hammer, C.U. and Spurk. M., 1996. Synchronised terrestrial-atmospheric deglacial records around the North Atlantic. *Science,* 274: 1155–1160.

Björck, S., Wohlfarth, B. and Possnert, G., 1995. ^{14}C AMS measurements from the Late Weichselian part of the Swedish Time Scale. *Quaternary International,* 27: 11–18.

Björck, S., Muscheler, R., Kromer, B., Andresen, C.S., Heinemeier, J., Johnsen, S.J., Conley, D., Koc, N., Spurk, M., and Veski, S., 2001. High-resolution analysis of an early Holocene cooling event suggest solar forcing as a major climate trigger. *Geology,* 29(12): 1107–1110.

Bond, G., Showers, W., Cheseby, M., Lotti, R., Almasi, P., deMenocal, P., Priore, P., Cullen, H., Hajdas, I., and Bonani, G., 1997. A Pervasive Millennial-Scale Cycle in North Atlantic Holocene and Glacial Climates. *Science,* 278(5341): 1257–1266.

Bond, G., Kromer, B., Beer, J., Muscheler, R., Evans, M.N., Showers, W., Hoffmann, S., Lotti-Bond, R., Hajdas, I., and Bonani, G., 2001. Persistent Solar Influence on North Atlantic Climate During the Holocene. *Science,* 294(5549): 2130–2136.

Borell, R. and Offerberg, J., 1955. *Geokronologiska undersökningar inom Indalsälvens dalgång mellan Bergeforsen och Regunda.* Sveriges Geologiska Undersökning, Ca 31: 1–24.

Bradley, R.S. and Jones, P.D., 1993. 'Little Ice Age' summer temperature variations: their nature and relevance to recent global warming trend. *The Holocene,* 3(4): 367–376.

Briffa, K.R., Jones, P.D., Schweingruber, F.H. and Osborn, T.J., 1998a. Influence of volcanic eruptions on Northern Hemisphere summer temperature over the past 600 years. *Nature,* 393: 450–455.

Briffa, K.R., Schweingruber, F.H., Jones, P.D., Osborn, T.J., Shiyatov, S.G., and Vaganov, E.A., 1998b. Reduced sensitivity of recent tree-growth to temperature at high northern latitudes. *Nature,* 391: 678–682.

Cappelen, J., 2002. *Yearly mean temperature for selected meteorological stations in Denmark, the Faroe Islands and Greenland; 1873–2001.* 02–06, Danish Meteorological Institute, Copenhagen.

Carlgren, M. *et al.*, 1925. *Skogsbruk och skogsindustrier i norra Sverige.* Almquist & Wiksells, Uppsala och Stockholm.

Cato, I., 1987. *On the definitive connection of the Swedish Time Scale with the present.* Sveriges Geologiska Undersökning, Ca 68: 1–55.

Cato, I., 1998. *Ragnar Lidén's postglacial varve chronology from the Ångermanälven valley, northern Sweden.* Sveriges Geologiska Undersökning, Ca 88: 1–82.

Chen, D., 2000. A montly circulation climatology for Sweden and its application to a winter temperature case study. *International Journal of Climatology,* 20: 1067–1076.

Chen, D. and Hellström, C., 1999. The influence of the North Atlantic Oscillation on the regional temperature variability in Sweden: spatial and temporal variations. *Tellus,* 51A: 505–516.

Cook, E.R., D´Arrigo, R.D. and Briffa, K.R., 1997. A reconstruction of the North Atlantic Oscillation using tree-ring chronologies from North America and Europe. *The Holocene,* 8(1): 9–17.

Crowley, T.J. and Lowey, T.S., 2000. How warm was the Medieval warm period? *AMBIO,* 19(1): 51–54.

Damon, P.E. *et al.*, 1998. Secular variation of the delta ^{14}C during the medieval solar maximum: a progress report. *Radiocarbon,* 40(1): 343–350.

D'Arrigo, R.D., Cook, E.R., Jacoby, G.C. and Briffa, K.R., 1993. NAO and sea surface temperature signatures in tree-ring records from the North Atlantic sector. *Quaternary Science Reviews,* 12: 431–440.

De Geer, G., 1912. A geochronology of the last 12,000 years. *Congrès de Geologie International, Comptes rendues:* 241–253.

De Geer, G., 1926. On the solar curve. *Geografiska Annaler,* 17: 253–283.

De Geer, G., 1940. *Geochronologia Suecica Principles.* Kungliga Svenska Vetenskapsakademiens Handlingar, 18(6): 1–367.

de Silva, S.L. and Zielinski, G.A., 1998. Global influence of the a.d. 1600 eruption of Huaynaputina, Peru. *Nature,* 393: 455–457.

Esper, J., Cook, E.R. and Schweingruber, F.H., 2002. Low-frequency signals in long tree-ring chronologies for reconstructing past temperature variability. *Science,* 295(5563): 2250–2253.

Fredén, C. (Editor), 1994. *Geology.* Sveriges National Atlas.

Gammelgaard, A., 2001. Hvor længe holder et 500 års dige? *Vejret,* 86: 27–38.

Gleick, P.H., 1989. Climate change, hydrology, and water resources. *Reviews of Geophysics,* 27(3): 329–344.

Haigh, J.D., 1996. The impact of solar variability on climate. *Science*, 272: 981–984.

Hansen, S., 1940. *Varvighed i Danske og Skaanske Senglaciale aflejringer.* Danmarks Geologiske Undersøgelse, II(63): 1–411.

Harlin, J., 1992. *Hydrological modelling of extreme floods in Sweden.* TRITA-VBI-159 Thesis, Royal Institute of Technonlogy, Stockholm, 358 pp.

Holmquist, B. and Wohlfarth, B., 1998. An evaluation of the Late Weichelian Swedish varve chronology based on cross-correlation analysis. *Geologiska Föreningen i Stockholm Förhandlingar,* 120: 35–46.

Hughen, K.A. *et al.*, 1998. Deglacial changes in ocean circulation from an extended radiocarbon calibration. *Nature*, 391: 65–68.

Hurrel, J.W., 1995. Decadal trends in the North Atlantic Oscillation: regional temperatures and precipitation. *Science*, 269: 676–679.

Jones, P.D., Briffa, K.R., Barnett, T.P. and Tett, S.F.B., 1998. High-resolution paleoclimatic records for the last millennium: interpretation, integration and comparison with general circulation model control-run temperatures. *The Holocene*, 8: 455–471.

Lamb, H.H., 1977. *Climate, present, past and future.* Meuhuen & Co Ltd, London.

Lambeck, K., Smither, C. & Ekman, M., 1998. Test of glacial rebound models for Fennoscandinavia based on instrumental sea- and lake-level records. *Geophysical Journal International,* 135: 375–387.

Lamoureux, S.F., 1999. Spatial and interannual variations in the sedimentation patterns recorded in nonglacial varved sediments of Canadian High Artic. *Journal of Paleolimnology,* 21: 73–84.

Leemann, A. and Niessen, F., 1994. Varve formation and the climatic record in an Alpine proglacial lake: calibrating annually-laminated sediments against hydrological and meteorological data. *The Holocene*, 4(1): 1–8.

Lidén, R., 1913. *Geokronologiska studier öfver det Finiglaciala skedet i Ångermanland.* 9, Sveriges Geologiska Undersökning.

Lidén, R., 1938. Den senkvartära strandförskjutningens förlopp och kronologi i Ångermanland. *Geologiska Föreningens i Stockholm Förhandlingar,* 60(3): 397–404.

Linderson, H., 2000. Conifer growth in the boreal forests of northern Sweden related to meteorological data. *Tiedonantoja,* 108: 25–35.

Lindström, G., 1993. *Floods in Sweden – trends and occurence.* RH No. 6, SMHI, Norrköping.

Lotter, A.F. and Birks, H.J.B., 1997. The separation of the influence of nutrients and climate on the varve time-series of Baldeggersee, Switzerland. *Aquatic Sciences:* 362–375.

Mann, E.M., Bradley, R.S. and Hughes, M.K., 1999. Northern hemisfere temperatures during the past millennium: inferences, uncertainties, and limitations. *Geophysical Research Letters,* 26(6): 759–762.

Mann, M.E., Bradley, R.S. and Hughes, M.K., 1998. Global-scale temperature patterns and climate forcing over the past six centuries. *Nature*, 392: 779–787.

McDermott, F., Mattey, D.P. and Hawkesworth, C., 2001. Centennial-scale Holocene climate variability revealed by a high-resolution speleothem δ18O record from SW Ireland. *Science*, 294: 1328–1331.

Milly, P.C.D., Wetherald, R.T., Dunne, K.A. and Delworth, T.L., 2002. Increasing risk of great floods in a changing climate. *Nature*, 415: 514–517.

Milthers, V., 1927. On the so-called Gothi-glacial limit in Denmark. *Geografiska Annaler Stockholm,* IX: 162–172.

Moberg, A., 1996. Meteorological observations in Sweden made before A. D. 1860. In: A. Moberg (Editor), *Temperature variations in Sweden since the 18th century.* Department of Physical Geography, Stockholm University, pp. 1–98.

Mörner, N.-A., 1996. Liquefaction and varve deformation as evidence of paleoseismic events and tsunamis. The autumn 10,430 BP case in Sweden. *Quaternary Science Reviews,* 15: 939–948.

Nilsson, B., 1972. *Sedimenttransport i Svenska Vattendrag ett IHD-Projekt, Del 2 Avrinningsområden, stationer och resultat 1967–69.* 16, Uppsala Universitet, Institutionen för Geovetenskab, Naturgeografi, Uppsala.

Oldfield, F., Crooks, P.R.J., Harkness, D.D. and Petterson, G., 1997. AMS radiocarbon dating of organic fractions from varved lake sediments: an empirical test of reliability. *Journal of Paleolimnology,* 18: 87–91.

Olsson, E., 1914. Översikt av de fasta fornlämningarna i Ångermanland. *Fornvännen:* 49–80.

Omstedt, A. and Chen, D., 2001. Influence of atmospheric circulation on the maximum ice extent in the Baltic Sea. *Journal of Geophysical Research,* 106(C3): 4493–4500.

O'Sullivan, P.E., 1983. Annually-laminated lake sediments and the study of Quaternary environmental changes – a review. *Quaternary Science Reviews,* 1: 245–313.

Palmer, T.N. and Räisänen, J., 2002. Quatifying the risk of extreme seasonal precipitation events in a changing climate. *Nature*, 415: 512–514.

Panagoulia, D., 1991. Hydrological response of a medium-sized mountainous catchment to climate changes. *Hydrological Sciences,* 36(6): 525–547.

Perkins, J.A. and Sims, J.D., 1983. Correlation of Alaskan varve thickness with climatic parameters, and use in paleoclimatic reconstructions. *Quaternary Research,* 20: 308–321.

Petterson, G., 1999. *Image analysis, varved lake sediments and climate reconstructions,* Ph.D. Thesis. Umeå University.

Petterson, G., Odgaard.B.V. and Renberg, I., 1999. Image analysis as a method to quantify sediment components. *Journal of Paleolimnology,* 22: 443–455.

Popper, K.R., 2002. *The logic of scientific discovery.* Routledge, 544 pp.

Raab, B. and Vendin, H. (Editors), 1995. *Klimat, sjöar och vattendrag.* Sveriges National Atlas.

Raisbeck, G.M. and Yiou, F., 1981. [10]Be in polar ice cores as a record of solar activity. In: R.O. Pepin, J.A. Eddy and R.B. Merrill (Editors), *The ancient sun.* Pergamon Press.

Richards, K., 1982. *Rivers form and process in alluvial channals.* Methuen, London and New York.

Rind, D., 2002. The Sun's role in climate variations. *Science*, 296: 673–677.

Rodwell, M.J., Rowell, P.D. and Folland, C.K., 1999. Oceanic forcing of the wintertime North Atlantic Oscillation and European climate. *Nature*, 398: 320–323.

Saarnisto, M., 1986. Annually laminated lake sediments. In: B.E. Berglund (Editor), *Handbook of Holocene Paleoecology and Paleohydrology*. Wiley, pp. 343–370.

Sander, M., Bengtsson, L., Holmquist, B., Wohlfarth, B. and Cato, I., 2002. The relationship between annual varve thickness and maximum annual discharge (1909–1971). *Journal of Hydrology*, 263: 23–35.

Schmutz, C., Luterbacher, J., Gyalistras, D., Xoplaki, E. and Wanner, H., 2000. Can we trust proxy-based NAO index reconstructions? *Geophysical Research Letters,* 27(8): 1135–1138.

Snowball, I., Zillén, L. and Gaillard, M.-J., 2002. Rapid early-Holocene environmental changes in northern Sweden based on studies of two varved lake-sediment sequences. *The Holocene,* 12(1): 7–16.

Strömberg, B., 1985. Revision of the lateglacial Swedish varve chronology. *Boreas*, 14: 101–105.

Stuiver, M. and Grootes, P.M., 1981. Trees and the ancient record of heliomagnetic cosmic ray flux modulation. In: R.O. Pepin, J.A. Eddy and R.B. Merrill (Editors), *The ancient sun*. Pergamon Press.

Stuiver, M. *et al.*, 1998. INTCAL98 Radiocarbon age calibration, 24.000–0 cal BP. *Radiocarbon*, 40(3): 1041–1084.

Svensmark, H. and Friis-Christensen, E., 1997. Variation of cosmic ray flux and global cloud coverage – a missing link in solar-climatic relationships. *Journal of Atmospheric and Solar-Terrestrial Physics,* 59(11): 1225–1232.

Wallin, J.E., 1996. History of sedentary farming in Ångermanland, northern Sweden, during the Iron Age and Medieval period based on pollen analytical investigations. *Vegetational History and Archaeobotany,* 5: 301–312.

Watson, R.T. and Coregroup (Editors), 2001. *IPCC Third Assessment Report: Climate Change 2001*. IPCC, Geneva, Switzerland, 184 pp.

Wohlfarth, B., 1996. The chronology of the Last Termination: a review of high-resolution terrestrial stratigraphies. *Quaternary Science Reviews,* 15(3): 267–284.

Wohlfarth, B., Björck, S., Cato, I. and Possnert, G., 1997. A new middle Holocene varve diagram from River Ångermanälven, Northern Sweden: indications for a possible error in the Holocene varve chronology. *Boreas*, 26: 347–354.

Wohlfarth, B. *et al.*, 1993. AMS dating Swedish varved clays of the last glacial/interglacial transition and the potential/difficulties of calibrating Late Weichselian 'absolute' chronologies. *Boreas*, 22: 113–128.

Wohlfarth, B., Holmquist, B., Cato, I. and Lindersson, H., 1998. The climatic significance of the clastic varves in Ångermanälven Estuary, northern Sweden, a.d. 1860 to 1950. *The Holocene,* 8.5: 521–534.

Wohlfarth, B., Possnert, G., Skog, G. and Holmquist, B., 1998. Pitfalls in the AMS radiocarbon-dating of terrestrial macrofossils. *Journal of Quaternary Science,* 13(2): 137–145

Wohlfarth, B. and Possnert, G., 2000. AMS ^{14}C measurements from the Swedish varved clays. *Radiocarbon*, 42(3): 323–333.

Xu, C.Y. and Halldin, S., 1997. The effect of climate change on the river flow and snow cover in the NOPEX area simulated by a simple water balance model. *Nordic Hydrology,* 28(4–5): 273–282.

Zillen, L.M., Wastegård, S. and Snowball, I., 2002. Calendar year ages of three mid-Holocene tephra layers identified in varved lake sediments in west central Sweden. *Quaternary Science Reviews,* 21(14–15): 1583–1591.

Zolitschka, B., 1992. Climatic change evidence and lacustrine varves from maar lakes, Germany. *Climate Dynamics,* 6(3–4): 229–232.

Zolitschka, B., Brauer, A., Negendank, J.F.W., Stockhausen, H. and Lang, A., 2000. Annually dated late Weichselian continental paleoclimate record from Eifel, Germany. *Geology*, 28(9): 783–786.